Plant Biotechnology Journal

WILEY | aab SEB

RESEARCH ARTICLE OPEN ACCESS

Gallic Acid-Responsive microRNAs Reprogram Lignification During Drought Acclimation Process in Spearmint

Alessia D'Agostino | Gabriele Di Marco | Gerardo Pepe | Adelaide Teofani | Chiara Pontecorvi | Manuela Helmer-Citterich | Antonella Canini | Angelo Gismondi

Department of Biology, University of Rome "Tor Vergata", Rome, Italy

Correspondence: Angelo Gismondi (gismondi@scienze.uniroma2.it)

Received: 13 October 2025 | **Revised:** 5 February 2026 | **Accepted:** 11 February 2026

Keywords: *Mentha spicata* | miRNome | phytostimulants | secondary cell wall modification | water deficiency

ABSTRACT

Mentha spicata L. (spearmint) is a high-value aromatic and medicinal species, whose productivity is strongly affected by water deficit. Nevertheless, the molecular mechanisms underlying drought acclimation in this mint remain largely unexplored. Thus, here, we investigated the microRNA-mediated regulatory processes triggered in *M. spicata* under drought stress (DS) and following treatment with gallic acid (GA), a natural phenolic compound that our research group has already documented to be a potential biostimulant for spearmint. A small-RNA sequencing approach revealed that both DS and GA induced substantial changes of the expressed miRNome, modulating 35 microRNAs (e.g., miR397a, miR159a, miR172b) whose predicted targets (e.g., Laccase-2, MYB transcription factors) are known to be involved also in lignin production. In detail, DS induced upregulation of lignin biosynthetic genes, enhancement of Laccase activity, and shifting in lignin monomer composition, promoting the putative reinforcement of the cell wall as expected during water deficiency. Conversely, GA treatment attenuated DS-induced stress, regulating microRNA-mRNA modules which balanced phytochemical and hormonal response while maintaining controlled lignification and optimising xylem function. These results highlight the pivotal role of microRNAs in orchestrating drought acclimation in *M. spicata* and identify GA as a compensatory agent under water-limiting conditions, capable of fine-tuning growth, cell wall remodelling, and redox homeostasis. Collectively, our findings provide molecular insights into biostimulant-mediated stress resilience and identify GA treatment as a promising biotechnological strategy to improve drought tolerance in Lamiaceae crops.

1 | Introduction

Spearmint (*Mentha spicata* L., Lamiaceae family) is a perennial herb cultivated worldwide for its remarkable aroma, pharmaceutical applications, and commercial value (Zhang, Chen, et al. 2022). This species generally requires frequent irrigation and adequate water supply (Marino et al. 2019); nevertheless, the knowledge of the effect of water stress on spearmint is limited so far (Delfine et al. 2005; Marino et al. 2019; D'Agostino et al. 2024).

MicroRNAs (henceforth miRNAs, miRs) are a class of small non-coding RNAs that play significant roles in plant organisms, influencing the gene expression at post-transcriptional or translational level. Although many aspects related to miRNAs still need to be clarified, it is known that these molecules are involved in various biological processes, in a time-, tissue-, genotype- and environment-dependent manner (Guleria et al. 2011; Zhang 2015; Begum 2022). For instance, their synthesis can be enhanced or suppressed in response to abiotic *stimuli*: thus, stress up-regulated miRNAs generally promote tolerance or

resistance phenomena, determining the protein silencing of their targets that act as negative regulators of plant acclimation (Chinnusamy et al. 2007). Vice versa, those downregulated by exogenous conditions typically target positive inducers of the plant response. According to this premise, working on miRNAs could represent a novel strategy for crop improvement (e.g., agronomic traits) and increasing plant productivity (Basso et al. 2019; Tiwari and Rajam 2022).

Drought has a significant impact on plant growth and yield; moreover, its effects are expected to intensify as global temperature rises. Thus, the comprehension of the molecular strategies underlying plant acclimation to such type of abiotic factor is fundamental for facing up to future challenges associated with climate change. Interestingly, drought has been identified to affect the expression of several miRNA families (e.g., miR172, miR396, miR397, miR398, miR408), whose role in this context requires further investigation being involved in ABA response, auxin signalling, osmoprotection, antioxidant defence, self-regulation of miRNA biogenesis pathway and lignification (Covarrubias and Reyes 2010; Ding et al. 2013).

Lignification, that is the generation of lignin in the cell wall, consists in the oxidative polymerisation of 3 types of phenylpropanoid units, known as monolignols (i.e., *p*-coumaryl alcohol, coniferyl alcohol and sinapyl alcohol) and synthesised from phenylalanine (Ralph et al. 2004; Vanholme et al. 2010). Cell wall-localised peroxidases, cinnamyl alcohol dehydrogenase and laccases are the enzymes involved in the final steps of production for this complex biopolymer (Sarkanen et al. 1991; Vanholme et al. 2010), although they may participate also in other biological processes. In particular, plant *LACCASE* genes (*LAC*s) have been documented to play important regulatory roles in cell elongation and pigmentation, beyond lignification of vascular and sclerenchyma tissues (Boerjan et al. 2003) which is essential for water transport, strength, and stress resilience. About the latter, for example, it has been demonstrated that drought leads to enhanced lignin deposition in the xylem vessels (Liu et al. 2018), suggesting that LACs activity is influenced by temperature and water deficiency. Therefore, coming back to the previous paragraphs, it is worthy of note the fact that several studies have showed how the expression of *LAC*s can be regulated by miRNAs, such as miR397 (Khandal et al. 2020; Huang et al. 2020), miR408 (Gao et al. 2022) and miR857 (Abdel-Ghany and Pilon 2008).

The application of exogenous substances to plants represents a biotechnological strategy to enhance crop growth, improve quality, optimise nutrient uptake, and increase stress tolerance (Bulgari et al. 2019; Drobek et al. 2019; Arslan et al. 2021). Thus, recently, our research team has proposed gallic acid (a natural trihydroxybenzoic acid; henceforth, GA) as a potential biostimulant for spearmint, enhancing its yield, quality, and drought acclimation capacity (D'Agostino et al. 2024), and for corn mint (*M. arvensis* L.), modulating positively its metabolome, especially the biosynthetic steps of menthol (D'Agostino et al. 2025). Starting from this point, the aim of the present contribution was to carry out a miRNome analysis on *M. spicata* plants subjected to GA and drought, to understand the possible contribution of miRNAs in triggering plant acclimation to water stress and to clarify if the suggested phytostimulant could favour this process. In addition, the pathway (i.e., lignification) which seemed to be mainly modulated by the miRNAs found differentially expressed among the samples was examined, proving evidence about its involvement in spearmint drought resilience.

2 | Results and Discussion

Drought is an adverse environmental condition inducing significant morphological, physiological, and molecular changes in plants, affecting crop production intensively (Liang, Yang, et al. 2024). Nonetheless, research investigating the impact of biostimulants on genes associated with drought resistance remains scarce and unclear. Thus, in the present contribution, the potential effect of GA, previously proposed as a phytostimulant (D'Agostino et al. 2024, 2025), and the involvement of miRNAs in the acclimation process of spearmint to water deficiency (DS) were investigated.

M. spicata plants were exposed to GA at the concentration of 50 μM (henceforth 50 μM GA), according to the best results obtained on this species by D'Agostino et al. (2024), and DS (henceforth CNT-DS), both singularly and in combination (50 μM GA-DS).

2.1 | Charting microRNA Landscape

Across all samples, small-RNA sequencing generated a total of 1 859 246 reads, corresponding to 35 distinct miRNAs. Their nucleotide sequences are listed in Table 1, along with the distribution of read counts for each of them across the different samples. The most abundant miRNAs were miR159a (951 344 total reads, tr), miR396e (390 070 tr), miR165a-3p (175 696 tr), and miR167d (102 752 tr). A Venn diagram (Figure 1, panel A) showed that 30 miRNAs were consistently expressed across all experimental conditions, while 5 were absent in at least one condition. Among them, miR398a-3p and miR164c-3p were not present in the CNTs, miR159b-5p was undetectable in 50 μM GA samples, whereas miR397a and miR169-d were lacking in 50 μM GA-DS.

To further examine the variation in miRNA expression and presence across the different experimental points, a principal component analysis (PCA) was performed (Figure 1, panel B). Although PC1 and PC2 explained 43% of the total variance, they displayed a partial separation of the treatments in three distinct clusters suggesting that GA may modulate the miRNA response to drought (I) containing just the CNT-DS, (II) with only 50 μM GA, and (III) presenting CNT and 50 μM GA-DS. This evidence indicates that GA or DS did not determine a specific signature on the samples exposed to respective type of treatment, but GA was able to change the miRNA profile induced by DS toward that shown by CNT plants.

MiRNA profiles obtained for all experimental conditions were visualised as a heatmap (Figure 1, panel C), with expression levels represented by a colour gradient ranging from white (low) to dark green (high). From the expressed miRNome analysis, it was evident that, compared to the control (CNT), both the drought-stressed samples (CNT-DS) and those exposed to the phytostimulant (50 μM GA) exhibited an overexpression

TABLE 1 | List of the expressed miRNAs. List of miRNAs identified by NGS analysis in the spearmint samples. For each of them, nucleotide sequence and number of raw sequencing reads counted in the various samples (in triplicate: _01, _02, _03) were also indicated.

miRNA	Sequence (5′–3′)	CNT_01	CNT_02	CNT_03	50 μM GA_01	50 μM GA_02	50 μM GA_03	CNT-DS_01	CNT-DS_02	CNT-DS_03	50 μM GA-DS_01	50 μM GA-DS_02	50 μM GA-DS_03
ath-miR159a	TTTGGATTGAAGGGAGCTCTA	103 790	26 730	57 031	80 765	105 806	88 065	115 562	35 319	198 462	48 497	20 559	70 758
ath-miR164a	TGGAGAAGCAGGGCACGTGCA	1626	525	597	1252	1338	1440	1614	666	3975	385	313	2262
ath-miR165a-5p	GGAATGTTGTCTGGATCGAGG	356	n.d.	94	126	274	96	499	93	725	198	43	940
ath-miR165a-3p	TCGGACCAGGCTTCATCCCCC	20 506	4557	7735	11 791	16 779	13 946	19 175	4981	39 764	8425	3162	24 875
ath-miR168a-5p	TCGCTTGGTGCAGGTCGGGAA	2267	597	464	997	1593	563	2315	401	4176	812	290	1938
ath-miR159b-5p	GAGCTCCTTGAAGTTCAATGG	8	n.d.	n.d.	n.d.	n.d.	n.d.	n.d.	n.d.	37	n.d.	3	6
ath-miR167d	TGAAGCTGCCAGCATGATCTGG	10 072	3160	5394	8019	10 328	10 227	14 012	3472	19 887	6261	2395	9525
ath-miR171b-3p	TTGAGCCGTGCCAATATCACG	n.d.	n.d.	3	n.d.	n.d.	96	176	n.d.	161	2	n.d.	59
ath-miR390a-5p	AAGCTCAGGAGGGATAGCGCC	157	n.d.	386	n.d.	468	290	154	37	265	103	76	127
ath-miR390a-3p	CGCTATCCATCCTGAGTTTCA	24	n.d.	243	n.d.	49	4	58	52	198	n.d.	51	72
ath-miR393a-5p	TCCAAAGGGATCGCATTGATCC	110	62	76	203	248	183	107	24	114	243	76	116
ath-miR396a-3p	GTTCAATAAAGCTGTGGGAAG	2093	731	1378	2206	2539	1098	2877	625	3385	1163	512	1715
ath-miR398a-3p	TGTGTTCTCAGGTCACCCCTT	n.d.	n.d.	n.d.	n.d.	n.d.	2	n.d.	n.d.	9	4	n.d.	13
ath-miR399a	TGCCAAAGGAGATTTGCCCTG	81	53	39	216	38	109	161	58	63	145	n.d.	94
ath-miR403-3p	TTAGATTCACGCACAAACTCG	3695	887	3083	3287	4854	3528	4925	1085	4989	2319	968	2806
ath-miR408-3p	ATGCACTGCCTCTTCCCTGGC	52	106	n.d.	n.d.	116	157	248	n.d.	78	51	n.d.	45
ath-miR164c-3p	CACGTGTTCTACTACTCCAAC	n.d.	n.d.	n.d.	42	34	58	102	45	27	n.d.	8	89
osa-miR156l-5p	CGACAGAAGAGAGTGAGCATA	40	3	3	n.d.	4	2	2	n.d.	9	n.d.	n.d.	8
ptc-miR172b-5p	GGAGCATCATCAAGATTCACA	n.d.	179	223	n.d.	135	47	n.d.	23	125	2	n.d.	42
ath-miR858a	TTTCGTTGTCTGTTCGACCTT	590	333	634	452	658	520	1200	201	2955	846	216	1290
ath-miR845b	TCGCTCTGATACCAAATTGATG	104	33	76	92	200	147	72	33	179	52	26	63
bna-miR171g	TGATTGAGCCGCGCCAATATCT	12	n.d.	43	98	n.d.	n.d.	43	15	42	24	n.d.	12
bna-miR397a	TCATTGAGTGCAGCGTTGATGT	40	106	73	n.d.	2	5	98	n.d.	20	n.d.	n.d.	n.d.
vvi-miR160a	TGCCTGGCTCCCTGAATGCCATC	369	337	421	134	80	396	329	135	714	119	19	433
vvi-miR172d	TGAGAATCTTGATGATGCTGCAT	247	n.d.	2	3	46	177	7	46	91	70	45	43
gma-miR172d	GGAATCTTGATGATGCTGCAGCAG	1903	457	799	1559	1926	1248	1547	423	3910	1829	528	1386
vvi-miR394a	TTGGCATTCTGTCCACCTCCAT	807	373	167	579	860	898	651	197	2609	508	301	1066

(Continues)

TABLE 1 | (Continued)

miRNA	Sequence (5′-3′)	CNT_01	CNT_02	CNT_03	50 μM GA_01	50 μM GA_02	50 μM GA_03	CNT-DS_01	CNT-DS_02	CNT-DS_03	50 μM GA-DS_01	50 μM GA-DS_02	50 μM GA-DS_03
sly-miR395a	CTGAAGTGTTTGGGGGAACTCC	62	n.d.	56	n.d.	114	35	132	7	197	46	n.d.	256
gma-miR156f	TTGACAGAAGAGAGAGAGCACA	4971	724	3181	1892	3378	4392	4662	732	8203	1683	935	3510
gma-miR169d	TGAGCCAAGGATGACTTGCCGGT	4	n.d.	n.d.	n.d.	2	n.d.	3	n.d.	n.d.	n.d.	n.d.	n.d.
gma-miR396e	TTCCACAGCTTTCTTGAACTGT	37813	14075	26452	34357	46318	37712	50488	13179	69376	17669	9594	33037
gma-miR166h-3p	TCTCGGACCAGGCTTCATTCC	4398	1117	1907	3190	3649	3821	5047	1729	7515	2335	770	4326
gma-miR167h	ATCATGCTGGCAGCTTCAACTGGT	46	20	34	n.d.	191	n.d.	40	43	40	53	44	10
gma-miR319i	TTGGACTGAAGGGAGCTCCTTC	595	185	930	1362	2150	1408	837	473	2988	2339	831	1128
gma-miR156r	CTGACAGAAGATAGAGAGCAT	95	n.d.	209	n.d.	59	282	99	41	352	245	60	79

Abbreviations: 50 μM GA, gallic acid treatment; 50 μM GA-DS, plants exposed to both gallic acid and drought stress; ath, *Arabidopsis thaliana*; bna, *Brassica napus*; CNT, control plants; CNT-DS, drought stress; gma, *Glycine max*; n.d., not detected or just 1 read counted; osa, *Oryza sativa*; ptc, *Populus trichocarpa*; sly, *Solanum lycopersicum*; Vvi, *Vitis vinifera*.

of distinct miRNA clusters, while the double-treatment determined a general downregulation of the miRNAs. The resulting hierarchical clustering from this graphical representation reinforces the outcomes of the PCA. Notably, CNT-DS plants showed the most pronounced differences in expression levels, with the highest values for nearly all the detected miRNAs. This observation aligns with previous studies, in which miRNAs have been documented to play a pivotal role in regulating plant defence mechanisms under stress conditions (Ferdous et al. 2015; Islam et al. 2022). Over-expression of well-known drought-responsive miRNAs (i.e., miR159b-5p, miR160a, miR168a-5p, and miR171b-3p) in spearmints subjected to water deficiency corroborates their putative contribution to stress tolerance even in *Mentha* genus (Liu et al. 2007; Eldem et al. 2012). Conversely, the downregulation or stabilisation of miR172b-5p and miR393a-5p in CNT-DS plants echoes previous findings that link the repression of these miRNAs with enhanced drought tolerance (Zhou et al. 2010; Eldem et al. 2012), presumably through the accumulation of their target mRNAs and the subsequent positive impact on stress adaptation. The 50 μM GA-DS samples displayed the fewest up-regulated miRNAs and clustered closely with the control (CNT), as already shown in PCA analysis, suggesting that GA alleviates drought-induced transcriptional stress. Plants treated with GA alone exhibited an intermediate profile, where a distinct cluster of miRNAs, namely miR167h, miR390a-5p, miR393a-5p, miR399a, and miR845b, resulted up-regulated. To date, no comparable study has examined whether GA or other phytostimulants trigger a similar miRNA spectrum, underscoring the novelty of these findings.

2.2 | miRNA-Mediated Resilience: Expression Dynamics During Drought and Gallic Acid Application

Among the 35 identified miRNAs, only eight were differentially expressed across the samples in a statistically significant way (henceforth DEMs, differentially expressed miRNAs): miR164c-3p, miR393a, miR160a, miR159a, miR172b-5p, miR858a, miR319i and miR397a. Their levels, as obtained by NGS data, were reported again in form of graph (Figure 1, panel D), together with their statistics. To validate these high-throughput results, the expression level of DEMs was further verified by qPCR assays (Figure 1, panel E). In parallel, to better discuss the trends shown by DEGs during the various treatments, the identification of their putative target genes was carried out using psRNATarget software. This was a critical step to understand the potential functions of the selected miRNAs and gain information about their regulatory roles in *Mentha spicata*. The results of this bioinformatics analysis were summarised in Table 2 (although the relative raw data were provided in full in Data S2).

The qPCR data were generally consistent with those from NGS (especially if one takes into consideration the significance), supporting the reliability of the sequencing approach, although the units of measure were different and the use of specific primer pairs for each miRNA makes qPCR analysis more sensitive and valid.

Sequencing analysis revealed an upregulation of miR164c-3p in all samples compared to the CNT, reaching its highest read

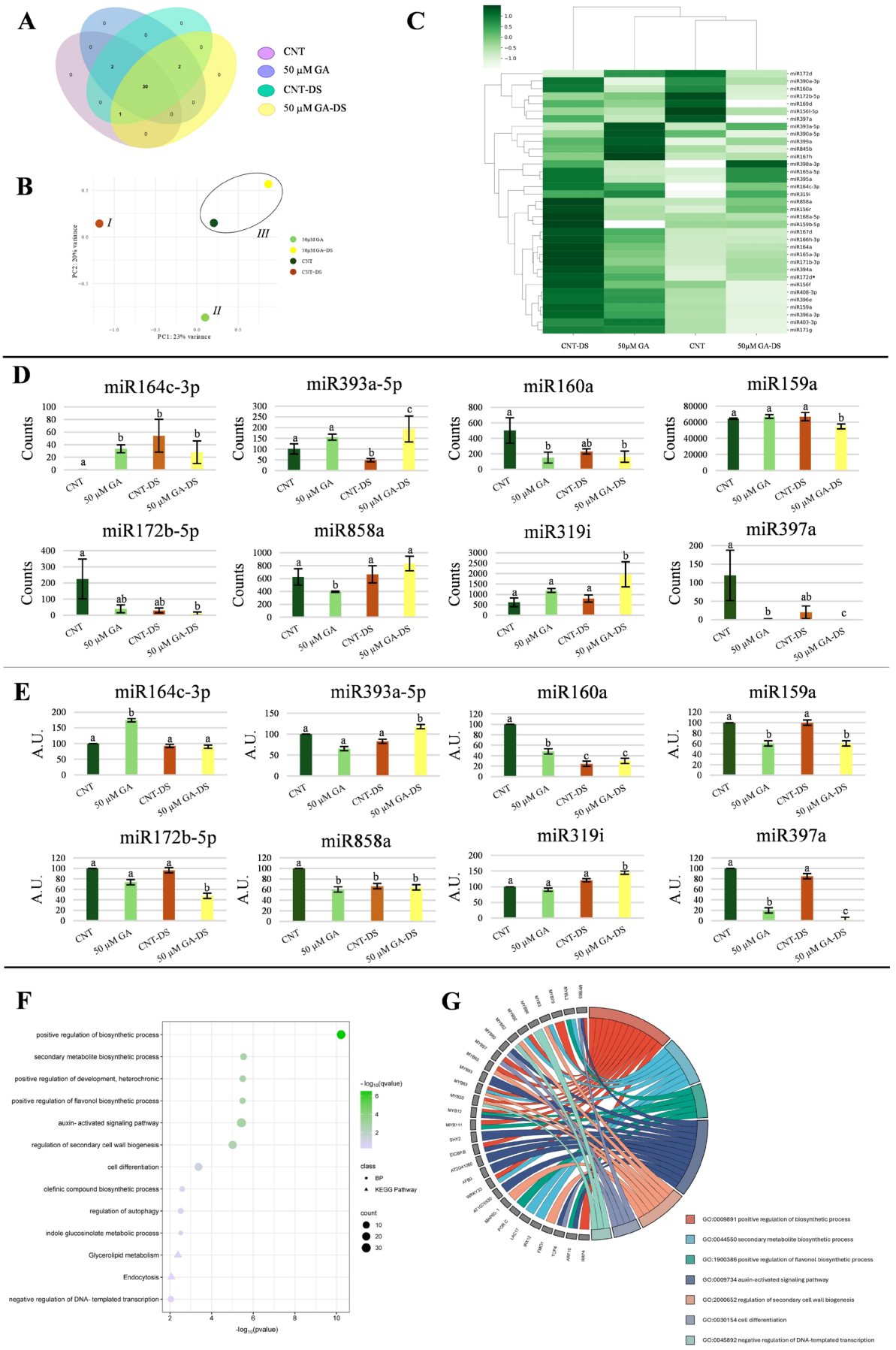

FIGURE 1 | Legend on next page.

FIGURE 1 | MiRNome analysis. (A) Venn diagram of expressed miRNA number in spearmint plants at each experimental condition. (B) PCA analysis of the miRNome profiles deciphered in each experimental set. The clusters identified in the graph were indicated with roman numbers (I, II and III). (C) Hierarchically clustered heatmap depicting miRNA expression profiles across the different spearmint samples; dark green represents high expression, while white low expression (according to *Z*-score scale with $p < 0.05$). Asterisk indicates gma-miR172d. (D) Histograms relative to sequencing data showing the counts of the 8 significantly DEMs among spearmint samples. (E) Histograms relative to qPCR data showing the relative abundance level (compared to CNT taken as unit, 100) of the 8 significantly DEMs among spearmint samples. (F) Results of the Gene Ontology (GO) enrichment analysis showing biological process and molecular function categories resulted for the list of all predicted targets for the 8 DEMs. The *x*-axis indicates the statistical significance [−log(*p*-value)], the colour provides information about multiple testing correction [−log(*q*-value)], while the bubble size reflects the counts of associated genes. (G) Pie chart showing the connections existing among the most significant targets of DEMs and the GO terms in which they are involved. All data in this figure are reported as mean ± standard deviation of three independent experiments. Different letters indicate significant statistical differences ($p < 0.05$).

count in the drought-stressed samples (CNT-DS; Figure 1, panel D). However, qRT-PCR showed that this increase was statistically significant only in plants treated only with the biostimulant (Figure 1, panel E), whereas CNT-DS and 50 μM GA-DS remained comparable to CNT plants. Our bioinformatic predictions identified members of the Protein Kinase Superfamily (PKS) as targets of this miRNA (Table 2). In support of this, in wheat, miR164 has been predicted and partially validated to be a post-transcriptional regulator of a Mitogen-Activated Protein Kinase (MAPK), that is indeed a member of PKS. These kinases are well known for their roles in pathogen-defence signalling as well as in mediating abiotic stresses, including water deficit (Wang et al. 2018). For example, the repression of miR164c-3p has been widely studied in the wild apple species, *Malus sieversii*, under water-deficit conditions (Peng et al. 2022). In that system, this miRNA seems to regulate No Apical Meristem (NAC) transcription factors, promoting the expression of reactive oxygen species (ROS) scavengers (e.g., peroxidases) and other abiotic defence genes. Anyway, the fact that this miR tends to accumulate, or to remain stable, in all treated spearmints indicates that maybe it does not play a key role during drought acclimation in *Mentha* species and that its presence could be eventually linked to the inhibition of unnecessary phosphorylation cascades or the promotion of oxidative bursts, usually associated to stress conditions (Mittler et al. 2022).

NGS data revealed that GA treatment induced a positive modulation in the expression of miR393a-5p in spearmint exposed to GA (Figure 1, panel D). Bioinformatic prediction identified the main targets for this miRNA as F-box proteins 3 and 2 (Table 2), core components of the auxin-signalling pathway that trigger AUX/IAA repressor degradation and thereby regulate plant development (Parry and Estelle 2006; Windels et al. 2014). Historically, miR393 has been shown to dampen auxin signalling by directing the cleavage of transcripts encoding auxin receptors, a mechanism repeatedly documented in drought acclimation (Chen et al. 2012; Lu et al. 2018). Its over-expression in GA samples would down-regulate auxin response, promoting the reshape of plant growth even under water deficit (Ferdous et al. 2015; Morad-Talab and Hajiboland 2016). This evidence could give support to the protective effect of GA against DS in spearmint, as already observed in D'Agostino et al. (2024). In addition, it is important to report that the same miRNA has been reported to be also inducible by abscisic acid (ABA), cold, and salinity stresses (Sunkar and Zhu 2004; Navarro et al. 2006). The decrease of miR393a-5p observed in CNT-DS, instead, could be an index of a release in auxin signalling, fostering even in this case growth and stress acclimation (Shi et al. 2014). Indeed, a similar response to drought has been reported in peach by Eldem et al. (2012), underscoring the context-dependent nature of this miRNA's regulation. Anyway, qRT-PCR demonstrated that only the co-treatment (50 μM GA-DS) significantly augmented miR393a-5p concentration. This result supports the hypothesis that GA attenuates miR393a-5p levels, which tended to decrease in the presence of water deficiency, to near-control values, hinting at a homeostatic adjustment, although further analyses would be needed to confirm a restoration effect.

Both NGS and qPCR analyses indicate that GA and drought stress significantly reduced miR160a expression in spearmint leaves (Figure 1, panels D and E). Bioinformatic predictions identify Auxin Response Factor 17 (*ARF17*) as a key target for this miRNA (Table 2), suggesting that the accumulation of this protein was favoured by both treatments. Indeed, miR160 has previously been reported to regulate leaf development under drought conditions, through its involvement in auxin signalling pathways (Yang et al. 2019). This regulation often occurs in conjunction with miR393 (Mallory et al. 2005; Liang, Chen, et al. 2024), targeting *ARFs* which specifically bind to auxin-responsive elements within promoter regions, thereby activating or repressing gene expression (Şanlı and Öztürk Gökçe 2021). Moreover, *ARFs* can interact with AUX/IAA proteins to form dimers, whose function is modulated by auxin levels (Hao et al. 2022).

Among drought-responsive genes, MYB transcription factors play pivotal roles; indeed, they control downstream targets essential for drought adaptation (Samad et al. 2017). Several *MYB* family members are known to be miRNA-regulated (Sunkar et al. 2012) and involved in the ABA-mediated pathways that control water loss tolerance (Reyes and Chua 2007; Khan et al. 2018). Based on our analyses, miR159a appeared to negatively regulate *MYB101* transcripts (Table 2), and its expression levels (Figure 1, panels D and E) remained fairly stable across most treatment conditions. Interestingly, NGS data revealed a significant reduction of its expression in the 50 μM GA–DS samples, while qPCR validation indicated a similar decrease in all plants treated with GA (with or without DS). In spearmint, we have previously observed that ABA levels significantly increased in drought-stressed (DS) plants, but the highest ABA concentration has been recorded under 50 μM GA-DS treatment (D'Agostino et al. 2024), a phenomenon which may contribute to stomatal closure and transcriptional regulation of stress-responsive genes. Taken together, these findings suggest that *M.*

TABLE 2 | Bioinformatics analysis by psRNATarget software. For each investigated miRNA (Query), the putative target mRNAs showing the lowest expectation value (Exp) were listed, both in the form of TAIR ID—The Arabidopsis Information Resource ID (Accession) and in full (Description). The complete output of the bioinformatics analysis here summarised is reported in Data S1.

		Target	
Query	**Exp**	**Accession**	**Description**
miR159a	2.0	AT2G32460.2	Myb domain protein 101
	2.0	AT2G32460.1	Myb domain protein 101
miR393a-5p	2.0	AT1G12820.1	Auxin signalling *F*-box 3
	2.0	AT3G26810.1	Auxin signalling *F*-box 2
miR858a	2.5	AT5G35550.1	Duplicated homeodomain-like superfamily protein
	2.5	AT5G35550.2	Duplicated homeodomain-like superfamily protein
	2.5	AT3G08500.1	Myb domain protein 83
	2.5	AT1G34670.1	Myb domain protein 93
miR397a	2.5	AT2G29130.1	Laccase 2
miR319i	3.5	AT5G64510.1	Tunicamycin induced protein
miR160a	2.0	AT1G77850.1	Auxin response factor 17
	2.0	AT1G77850.2	Auxin response factor 17
miR172b-5p	3.0	AT1G79730.1	Hydroxyproline-rich glycoprotein family protein
	3.0	AT2G37840.3	Protein kinase superfamily protein
	3.0	AT2G37840.1	Protein kinase superfamily protein
	3.0	AT2G37840.2	Protein kinase superfamily protein
	3.0	AT5G16730.1	Weak chloroplast movement under blue light protein
miR164c-3p	3.0	AT3G01490.2	Protein kinase superfamily protein
	3.0	AT3G01490.1	Protein kinase superfamily protein

spicata exhibits innate drought tolerance and that GA treatment may influence the miR159a-*MYB* module, potentially promoting ABA biosynthesis and enhancing stress adaptation mechanisms. Additionally, consistent with the proposed GA–miR159 regulatory axis, this miRNA would also bind the transcripts of *GAMYB*-like genes (*MYB33* and *MYB65*), promoting their degradation or translational inhibition. These factors, by mediating gibberellin signalling, drive developmental processes. In fact, their up-regulation would promote programmed cell death events linked to xylem production, which is made up of empty cells whose cell wall is enriched with lignin. Indeed, this reinforcement would increase the rigidity of vascular tissues, optimising water-use efficiency and contributing to drought tolerance (Li et al. 2016; Millar et al. 2019; Liu et al. 2020). Lastly, Li et al. (2016) have proved that *GAMYB*-like genes repression by miR159 is robust and not perturbated by a wide range of stresses, including water deficiency, justifying the stable level of this regulator in samples subjected to drought.

MiR172b-5p expression levels decreased significantly only in GA-DS treated samples (Figure 1, panels D and E). psRNATarget identified as putative targets for this miRNA the following factors: (i) members of the hydroxyproline-rich glycoprotein (HRGP) family; (ii) members of the protein kinase superfamily; (iii) the WEAK CHLOROPLAST MOVEMENT UNDER BLUE LIGHT protein (WEB1) (Table 2). Hydroxyproline-rich glycoproteins are plant cell-wall proteins characterised by abundant and often glycosylated hydroxyproline residues. They play crucial roles in cell-wall structure, integrity, and signalling throughout plant development (Showalter et al. 2016). Within this superfamily, proline-rich proteins are lightly glycosylated and interact with polysaccharides and other wall proteins, whereas extensins form a protein scaffold on which peroxidases oxidise monolignols. Indeed, the tyrosine-rich motifs of extensins undergo oxidative cross-linking in the presence of H_2O_2, generating nucleation sites for lignin assembly and stiffening the cell wall. Drought stress is known to trigger an immediate burst of ROS in the cell wall, which both cross-links extensins and stimulates peroxidase-mediated lignification. Thus, the extensin network reduces wall porosity, while a rapid lignin deposition limits water loss and enhances mechanical strength (Liang et al. 2020). The protein kinase superfamily comprises enzymes capable of transferring the γ-phosphate from ATP to specific amino acid residues on target proteins, thereby modulating enzymatic activity, subcellular localization, and interaction networks (Hanks and Hunter 1995). psRNATarget-based predictions indicate that miR172b-5p may recognise certain members of this family, introducing a post-transcriptional layer of control in kinase-mediated signalling pathways (Jones-Rhoades and Bartel 2004; Dai et al. 2018). By fine-tuning the expression of select kinases, miR172b-5p could indirectly influence cell-wall remodelling, hormonal crosstalk, and ROS dynamics under drought or high-light conditions. This intricate regulatory framework suggests that miR172b-5p extends beyond developmental phase control, engaging stress-responsive kinase networks and contributing to the biostimulant-enhanced drought tolerance observed in spearmint. Taken together, all this evidence suggests that the combination of GA and DS treatments could favour a possible strengthening and/or lignification process at the expense of the cell wall in spearmint. Additionally, according to the literature,

the canonical role of WEB1 is associated with light-mediated chloroplast movement (Kodama et al. 2010) and, to date, no studies have linked it to lignin biosynthesis or drought tolerance. However, light-dependent regulation of ROS in chloroplasts could modulate the phenylpropanoid pathway, potentially affecting lignin polymerisation under stress conditions. Altered chloroplast positioning might also impact local energy and redox homeostasis, thereby indirectly influencing monolignol biosynthesis and supporting the hypothesis previously formulated. In addition, it is known that chloroplasts adopt anticlinal orientations to minimise photo-oxidative damage and to optimise limited light and water use, and that their repositioning may activate cell-wall reinforcement pathways, including *NAC* and *MYB* transcription factors that drive lignification for enhancing mechanical strength and water retention (Zhong et al. 2011; Zhao and Dixon 2011; Choi et al. 2023). Finally, Wu et al. (2009) have reported that increasing miR172 levels promoted the appearance of adult traits, including the formation of trichomes on abaxial leaf surfaces. Based on previous evidence (D'Agostino et al. 2024), *M. spicata* maintains a constant trichome density after exposure to 50 μM GA and DS, reflecting the stable levels of miR172b-5p detected in the current work between CNT, CNT-DS and 50 μM GA conditions.

NGS and qPCR showed a different trend for miR858a: the omics approach revealed a decrease of this miR just in 50 μM GA samples, while the second method demonstrated that all treatments were effectively able to induce its reduction (Figure 1, panels D and E). Bioinformatic prediction identified duplicated homeodomain-like superfamily protein and MYB domain proteins 83 and 93 as putative targets (Table 2). The former constitutes a class of DNA-binding proteins involved in various developmental processes; for example, *CcBLH6* can regulate lignin deposition, a process usually activated in presence of drought (Yan et al. 2021). *MYB83* is regarded as an activator of the *NAC012/SND1*-mediated network, which regulates genes for cellulose, xylan, and lignin synthesis (McCarthy et al. 2009). Similarly, *MYB93* is a transcription factor involved in lignification and induced by ABA and auxin. Specifically, in apple, *MYB93* contributes to suberin deposition, another type of cell wall modification related to stress resilience (Legay et al. 2016). Based on these observations and considering the high specificity of qPCR assays, it can be hypothesized that both drought stress and application of the phytostimulant, even in combination, are able to induce the biosynthesis of compounds enhancing secondary wall deposition. This aspect, indeed, is fundamental in plants requiring mechanical stability and water transport efficiency as compensatory responses to drought stress. Thus, the present evidence implies that GA may promote lignification processes as well as drought (Choi et al. 2023).

MiR319i resulted significantly up-regulated only in 50 μM GA-DS samples (Figure 1, panels D and E), and the bioinformatics prediction revealed that Tunicamycin-induced proteins could be its potential targets (Table 2). Drought stress, similarly to tunicamycin treatment, can trigger endoplasmic reticulum (ER) stress and the unfolded protein response (UPR) in plants. This stress leads to the accumulation of misfolded proteins, activating the UPR to restore ER homeostasis (Kim et al. 2022). The up-regulation of miR319i in this spearmint sample subjected to double treatment might indicate a reduction of misfolded proteins, suggesting a potential positive effect of GA on drought-stressed plants (Zhou et al. 2013). The slight but non-significant increase of miR319i observed in the CNT-DS sample (Figure 1, panel E) could reflect the fact that, in spearmint under drought, ER was active and uncorrupted, being particularly involved in the synthesis and trafficking of enzymes involved in lignin biosynthesis (e.g., necessary to limit water loss). MiR319i might also negatively regulate some key transcription factors, like TCP and NAC family members, that have been connected to cell wall reinforcement by Zhou et al. (2013), thus enhancing drought tolerance.

The last DEM to be discussed is miR397a, which was significantly modulated only in all GA-treated samples (Figure 1, panels D and E) and whose target was *LACCASE 2* transcript (Table 2). In the literature, miR397 is well established as a negative regulator of laccases (e.g., *LAC4*, *LAC17*), enzymes that participate in lignin biosynthesis and related biological processes (Zhang et al. 2013; Wang et al. 2014; Swetha et al. 2018). This miRNA is responsive to various abiotic pressures, including drought and low temperature (Zhou et al. 2010; Dong and Pei 2014), and may mediate regulatory mechanisms conferring tolerance to different stressors. However, Khandal et al. (2020) have demonstrated that in *Arabidopsis* roots, under water-deficit conditions, elevated levels of miR397b suppress *LAC2*, which exceptionally works as a negative regulator of lignin deposition, as also reported by Yu (2020). A previous study has demonstrated that xylem with reduced lignin content exhibits diminished water transport efficiency (Kitin et al. 2010). Thus, miR397b-mediated downregulation of *LAC2* may promote lignin accumulation in vascular tissues, enhancing water conservation during drought stress. This is in line with the results obtained in CNT-DS samples, where the level of miR397a is maintained high, put in evidence that GA may be a promoter of *LAC2* expression (Figure 1, panel E). However, variation in miR397 expression levels under drought stress across different genotypes and developmental stages suggests that plant response to water deficit is shaped by genetic background and stage-specific water demands. Moreover, it has been supposed that distinct regulatory networks might control miR397 activity at successive phases of growth. Anyway, the upstream signals and downstream effectors that are involved in miR397 regulatory module during drought acclimation remain poorly understood, thus requiring further elucidation (Huang et al. 2020).

2.3 | Navigating the miRNA Targetome: Identification of Key Regulatory Players by Predictive Analysis

Starting from the complete lists of DEMs' putative targets (Data S2), a gene ontology (GO) enrichment analysis was carried out, to interpret the high-throughput molecular data and to generate hypotheses about the potential role in biological pathways of the detected miRNAs. Thus, Metascape software was used to identify all statistically enriched terms from GO and KEGG databases. In the multigroup Bubble Plot (Figure 1, panel F) it is possible to observe, in a comparative manner, the representation of the multiple enriched terms. The results showed that the changes of the miRNomes expressed in the spearmint samples were linked to specific phenomena. First of all, a positive

regulation of biosynthetic processes was identified, including secondary metabolite production (especially flavonols and indole glucosinolates); in fact, the existence of a significant change in the metabolome of *M. spicata* after exposure to DS and GA has been already documented in D'Agostino et al. (2024). After all, this result was quite expected considering that phytochemicals are the main tools used by plants for replying to exogenous pressures (Di Marco et al. 2018). Then, terms like positive regulation of development, auxin-activated signalling pathway, regulation of secondary cell wall biogenesis and cell differentiation were found at high significance. As already reported above, drought is one of the main environmental stresses that stimulate plants to change their morphology, especially at root and leaf level, and to induce production and strengthening of xylem tissue, for favouring resistance and transportation of water (Chen et al. 2012; Choi et al. 2023). These processes intrinsically require the action of hormones (e.g., auxin), trigger cell death and deposition of lignin in the cell wall (e.g., to differentiate tracheary and vessel elements), and induce changes in organ orientation (e.g., development alterations) and isolation (e.g., cutin and suberin accumulation), explaining the second set of GO terms. In addition, the terms previously discussed and suggesting the synthesis of plant compounds could be also linked to this second group of functions, being lignin, cutin and suberin polymers of phenolics, terpenes and lipids (according to the case). Within the last group of less prominent terms, interestingly, two KEGG processes could be also found: glycerolipid metabolism and endocytosis. Glycerolipids, being involved in energy storage, construction and fluidity of cell membranes and cell signalling, could play crucial roles in mint response to drought and GA, while the endocytosis has been recently linked to phenomena of (mainly long-distance) communication in plants or between plants and other organisms (e.g., bacteria, fungi). In fact, some studies have proposed how plant miRNAs, proteins, chemicals and other substances can be transported within the plant body, or released in the environment, by nanovesicles (i.e., exosomes), which represent real carriers for information (named signalosomes) among distant tissues or vehicles to carry out cross-kingdom regulations (Shkryl et al. 2022; Subha et al. 2023).

Subsets of genes and GO terms emerged by the enriched analysis were selected, due to their significance, and correlated in a GO Chord Plot (Figure 1, panel G), to better visualise the molecular relationships existing among them. Multiple *MYB* isoforms were identified, some of which mapped to the same GO terms (e.g., *MYB65*, *MYB33*, and *MYB101* with positive regulation of biosynthetic process, auxin-activated signalling pathway and cell differentiation). In such cases, a representative isoform was chosen to avoid redundancy and to enhance interpretability (e.g., *MYB65*). Among all, four MYB transcription factors mapped to three GO terms (Figure 1, panel G). Starting from *MYB65*, whose correlations with GO terms were just described, it has been reported that this *GAMYB*-like transcription factor, in vegetative tissues, inhibits growth by reducing cell proliferation (Alonso-Peral et al. 2010). *MYB65* could be indirectly linked to auxin responses, since miR159, responsive to auxin levels, seems to regulate its expression. Its functional overlap with *MYB33* and *MYB101* influences ABA signalling, which often interacts with auxin pathways during stress responses and developmental transitions (Wyrzykowska et al. 2022). *MYB12* was associated with positive regulation of biosynthetic process, positive regulation of flavonol biosynthetic process, and auxin-activated signalling pathway. In fact, according to literature, auxin induces the expression of *MYB12*, which is a flavonol-specific regulator of phenylpropanoid biosynthesis, activating genes such as chalcone synthase and flavonol synthase (Lewis et al. 2011). This class of flavonoids possesses strong antioxidant activity, thereby enhancing tolerance to abiotic factors such as drought and oxidative stress (Nakabayashi et al. 2014; Wang et al. 2016, 2021). *MYB20*, instead, was linked to positive regulation of biosynthetic process, regulation of secondary cell wall biogenesis, and negative regulation of DNA-templated transcription. In accordance with this evidence, *MYB20* is a transcriptional regulator involved in lignin biosynthesis, promoting the activation of genes in the phenylalanine and lignin biosynthetic pathways that contribute to secondary cell wall formation (Geng et al. 2020), and in stress response, binding to genes encoding protein phosphatases that act as negative regulators of ABA signalling (Cui et al. 2013). The last transcription factor, *MYB63* mapped to positive regulation of biosynthetic process, secondary metabolite biosynthetic process, and regulation of secondary cell wall biogenesis. Indeed, this factor was shown to positively modulate lignin transcriptional activators in *Arabidopsis thaliana* (L.) Heinh., binding to AC elements and regulating genes involved in lignin biosynthesis but not those involved in cellulose or xylan production (Zhou et al. 2009).

EICBP.B and *WRKY33*, both involved in the response to drought stress, were found to be associated with two GO terms (Figure 1, panel G). *EICBP.B* mapped with positive regulation of biosynthetic process and auxin-activated signalling pathway. This is a calmodulin-binding transcription factor whose expression is induced by ethylene, a hormone that plays a role in abiotic stress responses, including drought. Ethylene and ABA pathways interact during drought responses, and calmodulin-binding transcription factors are known to influence ABA signalling (Daszkowska-Golec and Szarejko 2013; Liu et al. 2025). On the other hand, *WRKY33* was shared between the processes of positive regulation of biosynthetic process and secondary metabolite biosynthesis. This transcription factor acts as a key regulator both in the perception of water deficit and in the activation of protective transcriptional networks. *WRKY33* binds directly to W-box elements in the promoters of its target genes, modulating the expression of factors involved in cell wall biosynthesis (Zhen Li et al. 2021). It also contributes to stomatal closure, reducing transpiration water loss without completely halting photosynthesis (Wang et al. 2019). Moreover, its role extends to hormonal and redox regulation, enhancing ABA levels, promoting the expression of *SUPEROXIDE DISMUTASE* and *CATALASE* genes for ROS control, and interacting with MAP kinases to modulate transcriptional responses to drought stress (Hussain et al. 2021; Guo et al. 2022). Finally, *WRKY33* overexpression has been shown to increase proline, soluble sugars, and peroxidase activity, resulting in improved plant survival under severe drought conditions (Wang et al. 2013).

Two other transcription factors, TCP4 and ARF10, were both mapped to the biological process auxin-activated signalling pathway (Figure 1, panel G). The former activates *YUC5*, a key gene in auxin biosynthesis, integrating auxin and brassinosteroid signalling to promote hypocotyl elongation (Challa et al. 2016), while the latter, regulated by miR160, plays a central role in leaf

water loss regulation via stomatal development and aquaporin expression (Liu et al. 2016). More in detail, ARF10 binds auxin response elements in the promoters of its target genes, mediating auxin response (Ulmasov et al. 1999). According to the present results, *TCP4* also aligned with secondary metabolite biosynthetic process. This evidence is supported by the work of Arif et al. (2018), in which this factor enhanced the accumulation of alkaloid compounds in the hairy roots of *Lycium ruthenicum*. *ARF10*, on the other hand, correlated with positive regulation of flavonol biosynthetic process. From the literature, it is known that ARF10 binds directly to AuxRE elements within the flavonol synthase promoter, modulating auxin polar transport and favouring antioxidative defences. The involvement of flavonols in auxin transport homeostasis highlights a feedback loop in which auxin fine-tunes itself through ARF10-mediated flavonol synthesis (Cao et al. 2024).

Finally, *LAC17* was involved in the secondary metabolite biosynthetic process (Figure 1, panel G), maybe through its role in lignin biosynthesis which contributes to plant cell wall structure and function and is part of the phenylpropanoid pathway (Zhang, Shan, et al. 2022).

2.4 | Lignification in Spearmint as Acclimation Response to Drought

Overall, miRNome analysis and bioinformatic predictions highlighted in spearmint samples exposed to drought and GA the modulation of several conserved miRNA-mRNA modules, widely discussed in the previous paragraphs (e.g., see miR858a, miR397a, miR172b-5p, miR159a), converging on the lignification process. This evidence was not so unexpected because, as stated above, the reinforcement of xylem tissue is recognised as an adaptive strategy to drought, enhancing resistance to hydraulic collapse and facilitating water transport (Choi et al. 2023; Yadav and Chattopadhyay 2023). Thus, the last part of the current study aimed at investigating this phenomenon.

In particular, the module miR397a-*LAC2* was explored in detail, since laccases are a family of cell wall-localised multicopper oxidases primarily involved in lignin biosynthesis (Bonawitz and Chapple 2010; Vanholme et al. 2010). It has been documented that miR397b overexpression reduces lignification in the vascular and interfascicular tissues of stems by negatively regulating the expression of several laccases (Arcuri et al. 2020; Gaddam et al. 2022). However, this molecular mechanism strongly depends on the studied plant species. Indeed, some laccases (e.g., *LAC10*, and *LAC17*) works polymerising lignin monomers, while others represent degradative isoforms (e.g., *LAC2*) (Khandal et al. 2020; Yu 2020). In this regard, it is important to mention that laccases belong to a moderately sized multigene family, counting, for instance, 17 genes in *Arabidopsis thaliana* (Turlapati et al. 2011), 49 genes in *Populus trichocarpa* (Lu et al. 2013), and 23 genes in *Phyllostachys edulis* (Li, Pang, et al. 2020). Anyway, to date, the precise number of laccases in *Mentha* genus is not available, making the information collected in this paper highly informative.

Considering all this premise, three laccases (i.e., *LAC2*, *LAC10* and *LAC17*) were selected and their mRNA level measured by qPCR in the spearmint samples (Figure 2, panels A, B, and C). The results showed that only the expression profile of LAC2 (Figure 2, panel A) seemed to be truly influenced by miR397a, presenting trends exactly inverted (Figure 1, panel E). GA-induced *LAC2* overexpression could be associated with modifications of xylem architecture, due to the negative role of *LAC2* on lignin deposition (Khandal et al. 2020; Sharma et al. 2020; Yu 2020), though its net effect on drought tolerance may vary depending on species and environmental conditions (Niu et al. 2021). Interestingly, the applied biostimulant appeared to induce an upregulation of *LAC10* transcript but not of *LAC17* (Figure 2, panels B and C), whose expression was quite totally nullified. However, both these mRNAs rose significantly under water-deficit conditions (CNT-DS), by 4585.07% and 202.09% respectively, compared to the CNT. This result indicates that both LAC10 and LAC17 are enzymes strongly activated during drought stress, contributing to lignin polymerisation and cell-wall strengthening. Anyway, when water deficiency was associated to GA treatment (i.e., 50 μM GA-DS) only LAC10 resulted up-regulated with respect to the CNT (although at a less extent than CNT-DS). The present evidence could indicate a compensatory effect of GA on DS-stressed spearmints, which appeared able to reduce their basal defence mechanism of lignification, maybe triggering other response systems.

All this hypothesis was supported by a Western blotting analysis conducted to measure total Laccase (LAC) protein content (Figure 2, panel D). Densitometric quantitation showed that CNT-DS plant extract accumulated a high level of LAC (+497.5%), while the others obtained from GA-treated mints showed a stable level, with respect to CNT (Figure 2, panel E). As previously stated, different LACs work simultaneously, synergistically or antithetically, to remodel woody tissues (not only those here monitored by qPCR); therefore, it is difficult to determine which of them contributes most in our model system, in the absence of specific antibodies and given the still limited knowledge about the *Mentha* genome. For these reasons and to confirm the protective role of GA against drought stress in spearmint, other aspects of the lignification pathway were characterised in the present contribution.

Transcript or protein levels of an enzyme do not necessarily correspond always to its activity, due to the existence of several regulation levels (e.g., protein stability); thus, total laccase activity was assessed by a specific kit (Figure 2, panel F). The highest activities were recorded in the CNT (864.1 mU/mg) and CNT-DS (664.3 mU/mg) samples. While the result relative to drought-stressed plants was expected as consistent with the Western blotting and gene expression analyses, the high functionality of LACs found in the CNT appeared quite unpredictable. However, laccases with potential degradative functions have been extensively studied in fungi but are poorly documented in plants. Therefore, this latter observation could be associated with their activity, also justifying the basal levels of degradative *LAC2* mRNA previously reported (Figure 2, panel A). On the other hand, the reduced LAC activity observed in GA-exposed samples might be related to the ability of the phytostimulant to trigger biochemical and hormonal signals resulting in this sense. Indeed, GA might promote the synthesis of antioxidant molecules in spearmint, as demonstrated by D'Agostino et al. (2024), and/or improve photosynthetic efficiency, thereby reducing ROS

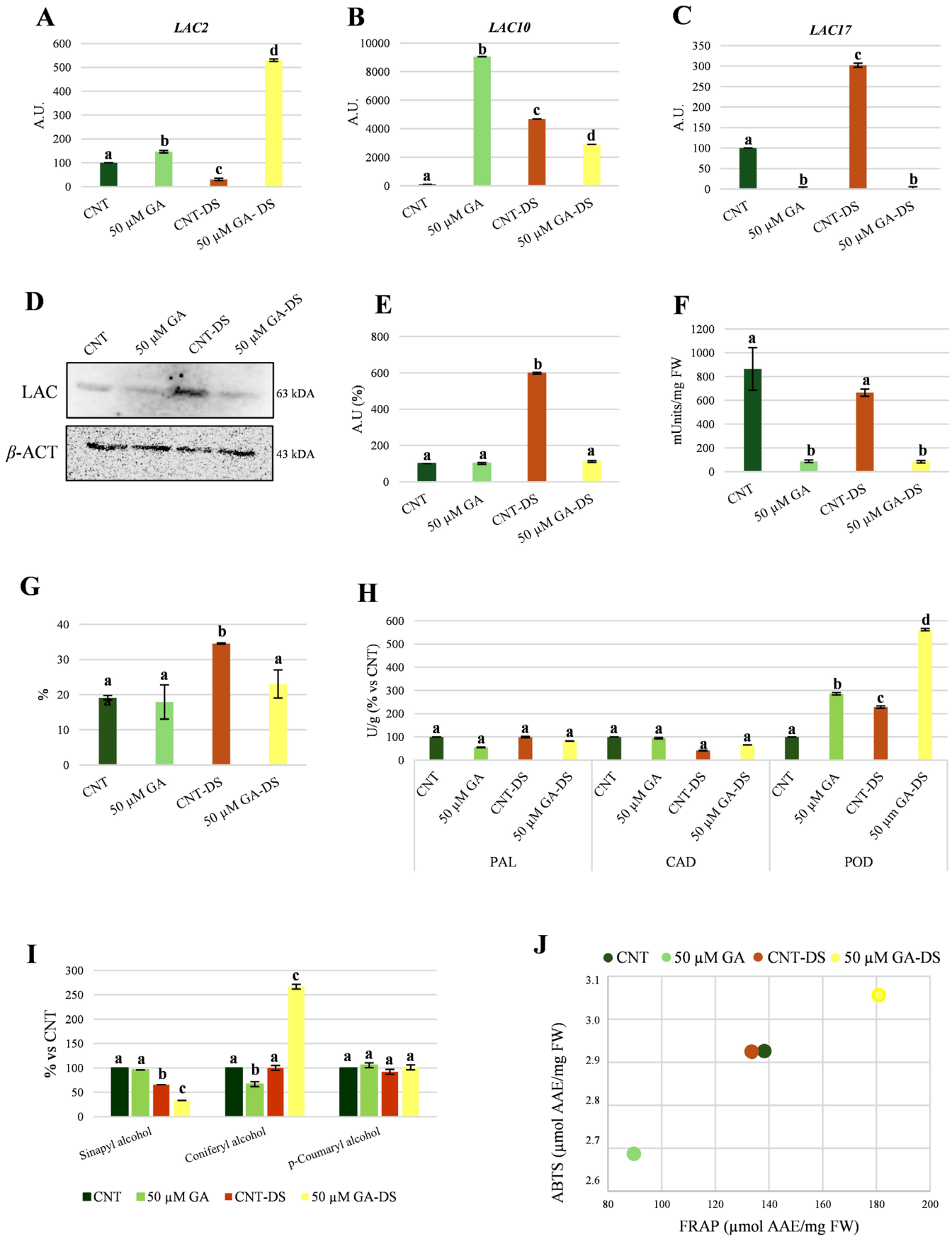

FIGURE 2 | Legend on next page.

FIGURE 2 | Lignification-related aspects. Graphical representation of real-time qPCR data representing the gene expression levels of: (A) *LACCASE2*, (B) *LACCASE10* and (C) *LACCASE17*. The mRNA levels were normalised with respect to *β-ACTIN* and expressed as arbitrary units (A.U.) compared to the CNT (considered as 100). (D) Representative immunoblots showing total LACCASE (LAC) and β-ACTIN (β-ACT, used as a loading control) protein signals (E) Results of the quantitation of the immunoblots reported in the panel D as percentage variation compared to the CNT taken as unit (100%). (F) Total LACCASE activity measured spectrophotometrically by a specific kit. (G) Total lignin content quantified by a specific kit and expressed as tissue percentage (%). (H) Activity of Phenylalanine ammonia-lyases (PAL), Cinnamyl alcohol dehydrogenases (CAD), and Peroxidases (POD) assessed by specific kits. (I) Histogram showing the content of monolignols (sinapyl alcohol, coniferyl alcohol and *p*-coumaryl alcohol) determined by HPLC-DAD analysis. (J) Antiradical potential of the plant tissues measured by FRAP and ABTS in vitro assays. In the graph, the two tests were correlated. All results in this figure are reported as the mean of three independent experiments ± standard deviation. Different letters indicate significant statistical differences ($p < 0.05$).

accumulation, a condition that normally upregulates laccases (Khandal et al. 2020).

Lignification is part of the normal differentiation programme of specific tissues but, in response to various abiotic stresses, can also be induced in cells that should not lignify to increase mechanical strength (Barros et al. 2015). In line with this declaration, the measurement of total lignin content supported the previous evidence, putting in evidence that only plants subjected to DS exhibited an increase in lignin amount, although only CNT-DS in a significant way (Figure 2, panel G).

In order to better figure out what was happening in the spearmint plants, the analysis of the activity of other enzymes involved in lignin biosynthesis was carried out (Figure 2, panel H). Among them, enzymes upstream of laccases, that is phenylalanine ammonia-lyase (PAL; it catalyses the deamination of L-phenylalanine into ammonia and *trans*-cinnamic acid, the common precursor for all phenolic derivatives) and cinnamyl alcohol dehydrogenase (CAD; responsible for the reduction of cinnamaldehydes—coniferyl, sinapyl, and *p*-coumaraldehyde—to their corresponding monolignol alcohols), and others that works in parallel with them (i.e., peroxidases, henceforth PODs) (Gayoso et al. 2010; Vanholme et al. 2010; Liu et al. 2018). It is important to underline, in fact, that the oxidative polymerisation of monolignols (i.e., sinapyl alcohol in syringyl S unit; coniferyl alcohol in guaiacyl G unit; *p*-coumaryl alcohol in *p*-hydroxylphenyl H unit), generating radicals that combine to form the lignin network in the secondary cell wall compartment (Liu et al. 2018), do not occur only at the expense of LACs but depend also on PODs, providing a further key for interpreting the previous data. In all samples, PAL and CAD activity remained constant compared to the CNT, whereas POD was hyperactivated. This finding aligns with previous reports showing that enhanced drought tolerance is linked to increased ROS-scavenging enzyme activity and expression, such as PODs (Zhang and Kirkham 1994; Sharma et al. 2012; Peng et al. 2022). Interestingly, it seemed that a more pronounced increase of the activity for these enzymes could be registered under GA treatment (+185.71% in 50 μM GA; +471.9% in 50 μM GA-DS).

Analysis of monolignols by HPLC-DAD revealed significant changes in sinapyl alcohol and coniferyl alcohol levels (Figure 2, panel I), while *p*-coumaryl alcohol content remained constant across all treatments. It is well documented that lignin composition varies among plant species and tissues. In dicotyledonous plants, for example, lignin in tracheary elements is mainly enriched in guaiacyl (G) units (Weng and Chapple 2010; Pesquet et al. 2019). In *M. spicata*, under water deficiency, sinapyl alcohol levels tended to decline, suggesting a possible specific effect of this stress on the production of S units. By contrast, coniferyl alcohol (then G units) concentration remained unchanged between CNT and CNT-DS, decreased by 34% under GA treatment alone but, curiously, significantly increased (by 166.7%) compared to the CNT when drought and GA were combined. Syringyl (S) units are preferentially incorporated during the late stages of cell-wall maturation, and an increase in G unit content has been registered in *Eucalyptus* plants subjected to water deficit, together with a reduction in the S/G ratio, validating the data reported in the present work (Moura-Sobczak et al. 2011). In spearmint, GA might accelerate cellular development under drought conditions, thereby elevating coniferyl alcohol accumulation. Moreover, G-rich lignin is more condensed, hydrophobic, and rigid, properties that reinforce cell walls and minimise water loss. Thus, the double treatment (GA-DS) likely drives the plant to invest in G deposition to optimise mechanical strength and enhance its barrier against dehydration.

As final step of the research, the antioxidant activity of the spearmint samples was measured by two different assays, ABTS and FRAP, and the values obtained correlated in a single graph (Figure 2, panel J). The mean FRAP and ABTS values for CNT and CNT-DS plants were nearly identical (138.54 μmol AAE/mg for CNT vs. 133.82 μmol AAE/mg for CNT-DS in FRAP test; 2.925 μmol AAE/mg for CNT vs. 2.921 μmol AAE/mg for CNT-DS in ABTS test). Consequently, both samples clustered together toward the centre of the plot. Among all, 50 μM GA plants showed the lowest antiradical power during both tests. This could be justified by the fact that, as documented in D'Agostino et al. (2024), the level of ROS (i.e., hydrogen peroxide and superoxide anion) was reduced in the spearmint tissues exposed to phytostimulant at this specific concentration. Therefore, by decreasing the level of reactive species, the need for an antioxidant-rich intracellular environment may also be diminished. A similar result was also observed for 50 μM GA-DS sample but the antiradical assays, by contrast, revealed strong signals. Maybe, the combination of the two treatments may have stimulated the activation of further redox defence mechanisms, such as the synthesis and accumulation of antioxidant molecules (e.g., phenolic compounds, as reported by D'Agostino et al. 2024), with potential positive implications for the extract's functional value.

3 | Conclusions

The present study represents the first characterisation of *M. spicata* expressed miRNome under drought conditions and gallic

acid application, providing evidence for a key involvement of miRNAs in the modulation of stress-responsive pathways. Differential expression analysis, carried out by small-RNA sequencing and qPCR assays, identified conserved plant miRNAs whose predicted targets converge on lignification-related genes, with particular emphasis on Laccases, thereby indirectly supporting the hypothesis that even in this species secondary cell wall reinforcement constitutes a major acclimation strategy to water deficit. The observed reprogramming of miRNA expression profiles in GA-treated plants indicates that this phenolic compound may contribute to mitigating drought-induced molecular response, possibly aligning regulatory networks toward a transcriptional state closer to controls. Such modulation may be associated with a change in lignin deposition, while potentially sustaining redox homeostasis and hormone-mediated signalling, contributing to drought resilience. Collectively, these findings extend current knowledge on miRNA-associated regulation of stress responses in Lamiaceae species and propose GA as a potential candidate phytostimulant for improving crop performance under limited water availability. Future work should aim at validating the other identified miRNA-mRNA modules through functional assays and exploring their stability across genotypes and other environmental scenarios.

4 | Experimental Procedures

4.1 | Plant Material, Growth and Stress Conditions

The plant material was the same described and used in D'Agostino et al. (2024). Briefly, one-month-old spearmint plants (*Mentha spicata* subsp. *spicata* L.) were obtained from a guaranteed provider and divided into two groups: control (CNT) and test. Pure gallic acid (GA; Sigma-Aldrich) was mixed with the mineral soil of the test plants, following the evidence from available literature and preliminary laboratory tests (8.50 mg per Kg of soil; henceforth, 50 μM GA). A set of control and test plants (henceforth, CNT and 50 μM GA) was irrigated daily to maintain a water level equal to 85% of the field capacity (FC), while another set was subjected to a regime of drought stress (henceforth, DS; CNT-DS and 50 μM GA-DS) consisting of suboptimal watering (42.5% FC). In detail, the 100% FC was determined gravimetrically by saturating the soil and allowing it to drain for 24 h until constant weight. The water content was checked twice per day by weighing the whole pot (including plant, soil, and pot) and replenishing the water lost to reach the target FC percentages (see D'Agostino et al. 2024 and literature within). The experiment was carried out for 21 days (temperature: 22°C; photoperiod 14 h light/10 h dark; homogeneous light intensity: 120 $\mu mol\, m^{-2} s^{-1}$); then, the plant material was collected, powdered with pestle and mortar in presence of liquid nitrogen and stored at −80°C until the analyses. Each experimental point consisted of 6 plants (independent biological replicates).

4.2 | MicroRNA Isolation

MirPremier microRNA Isolation Kit (Sigma-Aldrich, St. Louis, USA) was used according to the manufacturer's guidelines to purify miRNAs from *M. spicata* powdered plant material. Quality and concentration of miRNAs were determined using a NanoDrop 2000 spectrophotometer (Thermo-Fisher Scientific, USA). To check the absence of nucleases during the procedure and the reliability of the extraction method, qRT-PCR assays were performed, as reported in Gismondi et al. (2017) (for further details see next paragraph), using the cDNA retro-transcribed from the isolated miRNAs as template and a StepOnePlus instrument (Perkin-Elmer Applied Biosystems) as Real-Time PCR System. In particular, the presence of UniSp6 (a synthetic RNA molecule added to cDNA samples and used as an internal control of the retro-transcription step, QIAGEN), miR159a (a ubiquitous and abundant plant miRNA; miRBase accession number: MI0023002; miRCURY LNA miRNA PCR Assays) and plant 5S rRNA (considered as positive control, developed and designed by EXIQON Service on the basis of plant 5S rDNA sequences *Arabidopsis thaliana* GenBank: AB073495.1; miRCURY LNA miRNA PCR Assays) was investigated, together with the incapacity to amplify the negative controls (Neg1, absence of template; Neg2 absence of primers). Agarose gel (1%; w/v) containing 10 mg/mL ethidium bromide was used to fractionate by electrophoresis the PCR products in the presence of TAE buffer (40 mM Tris; 1 mM EDTA; 20 mM acetic acid; pH 8.5). Amplicons were visualised under UV light (ChemiDoc Imaging Systems, BIO-RAD) and the positive samples were subjected to NGS analysis.

4.3 | Small RNA Sequencing

Indexed libraries were prepared with NEXTflex small RNA-Seq Kit v3 (Perkin Elmer), according to the manufacturer's instructions, from the pool of miRNAs previously isolated. Libraries were quantified using the Tape Station 4200 (Agilent Technologies) and Qubit Fluorometer (Invitrogen Co., Carlsbad, CA) and pooled such that all index-tagged samples were present in equimolar amounts. Sequencing was carried out using an Illumina Novaseq6000 System (Illumina platform) in a 2×75 paired-end format.

4.4 | miRNome Profiling

Raw sequence files (.fastq files) obtained by sequencing underwent quality control analysis using FastQC software (v0.12.0) (Andrews 2010). Only sequences showing at least 80% of bases called with a quality score of 30 or higher were selected. Sequencing adapters were removed using Cutadapt (v2.8) (Martin 2011). After that, the reads were processed by trimming low-quality bases at their edges, using the BBDuk tool from BBMap and setting these parameters 'qtrim = rl' and 'trimq = 20'. Only reads ranging from 21 to 25 nucleotides (post adapter-removal) were kept, ensuring that only miRNA-derived reads were retained. Reads were aligned to miRBase (Kozomara et al. 2019) and, given that this database includes identical miRNAs from various species, the analysis was performed selectively on sequences classified under the section Viridiplantae, to mitigate alignment noise. To address the residual data redundancy, miRNA sequences were clustered based on a 90% sequence similarity threshold, identifying a representative miRNA for each cluster using CD-HIT software (v4.8.1) (Li and Godzik 2006). High-quality reads were further aligned to the Viridiplantae subset of miRbase, using BBMap aligner (Bushnell 2014) and employing parameters such as

'ambig = best', 'vslow', and 'semiperfectmode'. The counts of all miRNAs within each cluster were aggregated, normalised using DESeq2's median of ratios method and subjected to differential expression analysis, using the negative binomial generalised linear model included in DESeq2 (v1.42.0) (Love et al. 2014). Differentially expressed miRNAs (DEMs) were those showing a significant change among the samples, in terms of Z-score, associated to a $p < 0.05$. Principal Component Analysis (PCA) was performed using plotPCA tool of DESeq2. On the other hand, Venn diagram and heatmap, including the relative hierarchical clustering, were created, respectively, by ggvenn and Heatmap.2 functions from R gplots package. Finally, psRNATarget server (Dai and Zhao 2011) was applied to predict the mRNA targets for DEMs, which were used to carry out a Gene Ontology enrichment analysis by Metascape (http://metascape.org) (Zhou et al. 2019); the results were reported as chord and multigroup bubble plots generated via SRplot tool (Tang et al. 2023).

4.5 | Quantitation of microRNAs by qRT-PCR

Real time PCR (qRT-PCR or qPCR) was used to validate miRNome analysis and quantify miRNAs. Before starting, 1 μg of miRNAs were retro-transcribed to cDNA, as reported above. The experiment was performed in 10 μL of final reaction volume containing: 25 ng cDNA, 50% SYBR green (Kapa SYBR Fast qPCR kit; Kapa Biosystems, Woburn, MA, USA) and 1 μL of the mixture presenting both miRNA specific PCR primers (microRNA LNA PCR primer sets, QIAGEN). The amplification was performed using a StepOnePlus Real-Time PCR thermocycler with the following parameters: (a) initial denaturation at 95°C for 10 min; (b) 45 cycles of denaturation at 95°C for 15 s (sec) and primer annealing at 60°C for 1 min; (c) production of disassociation curve: 95°C for 15 s and then a ramp from 60°C to 95°C, with a rate of 0.3°C every sec. The expression of miRNAs was calculated through the $2^{-\Delta\Delta Ct}$ method, using 5S rRNA as internal reference gene, as reported in Gismondi et al. (2017). Data were calculated as mean ± standard deviation (S.D.) and expressed in percentage with respect to the CNT (considered as unit, 100%).

4.6 | RNA Extraction and Analysis

Total RNA was extracted with WizPrep Total RNA Kit (Wizbiosolutions, Loco Hills, United States), according to the manufacturer's guidelines, starting from 100 mg of frozen and powdered plant material. RNA was quantified by NanoDrop ND1000 spectrophotometer (NanoDrop Technologies) and stored at −80°C. cDNA was synthesised starting from 2.5 μg of RNA by WizScriptTM cDNA Synthesis Kit (High Capacity). Briefly, RNA was incubated for 10 min at 25°C with reaction buffer, dNTP mix, random hexamer (50 pM), 200 U/μL WizScript RTase, 40 U/μL RNA inhibitor, and RNase-free water (final volume of 20 μL). Then, the incubation period continued for 2 h at 37°C and 5 min at 85°C. cDNA samples were quantified and stored at −80°C until use. qRT-PCR assays were carried out by mixing 30 ng of cDNA, 50% SYBR Green PCR Master Mix (Perkin-Elmer Applied Biosystems, Waltham, MA, USA), and 5 pmol of forward and reverse primers (Data S1). The StepOnePlus Real-Time PCR System was used for the amplification and set as follows: 10 min at 95°C, followed by 45 cycles of 20 s at 95°C and 30 s at 59°C. The dissociation curve, instead, consisted in 95°C for 15 s, 60°C for 1 min and then a ramp toward 95°C at a rate of 0.3°C every 15 s. RNA levels were calculated using the $2^{-\Delta\Delta Ct}$ formula, using *β-ACTIN* as internal reference control, due to its stable expression in our plant samples (although also another housekeeping gene was checked: eukaryotic initiation factor 4A, *eiF-4A*). Data were calculated as mean ± standard deviation (S.D.) and expressed in percentage with respect to the CNT (considered as unit, 100%).

4.7 | Protein Extraction and Western Blotting

Plant powder (400 mg) was resuspended in 600 μL of ice-cold extraction buffer (25 mM Tris–HCl pH 7.5, 150 mM NaCl, 0.1% Triton X-100, 1 mM EDTA, 5 mM dithiothreitol, and 1X protease inhibitors cocktail). Samples were incubated for 15 min in ice and then centrifuged at 10000 *g* for 10 min at 4°C. The supernatant was centrifuged again at 13000 *g* per 30 min at 4°C and finally collected in a new tube. Protein concentration was estimated by the Bradford assay, using bovine serum albumin as standard, through a microplate reader (Sunrise, Tecan). According to Gismondi et al. (2013), proteins were separated in a 12% sodium dodecyl sulfate-polyacrylamide gel and transferred onto a Protran nitrocellulose membrane (Schleicher and Schuell). Blots were incubated with the following primary antibodies: rabbit polyclonal anti-β-ACTIN (AS132640; Agrisera AB, Sweden) and rabbit polyclonal anti-LACCASE (HPA040150; Merck, Milan, Italy). Finally, primary antibodies were revealed using horseradish peroxidase-conjugated anti-rabbit (A0545; Merck, Milan, Italy) and an ECL chemiluminescence detection system (Pierce). Signal acquisition and quantitation were carried out by ChemiDoc Imaging System (BIO-RAD) and LICORbio software (Image Studio v6.0, LI-COR Biotech).

4.8 | Enzymatic Assays

The activity of Laccases was measured by the Laccase Activity Assay Kit (ab284539; K2038, ABCAM), strictly following the guidelines provided by the manufacturer. One hundred mg of plant material were used for carrying out the test. The optical density (henceforth, OD) of the reaction mixture was measured spectrophotometrically at 420 nm using a spectrophotometer (microplate reader Sunrise, Tecan) and then expressed as unit of enzyme activity (or rather the amount of enzyme that produces 1 μmol of oxidised product per minute at pH 4 at 37°C) per milligram of fresh plant tissue (mUnits/mg FW). Phenylalanine ammonia-lyase (PAL) activity was evaluated following the protocol of the relative kit (BC0215, Solarbio Science and Technology Co. Ltd., Beijing, China). A total of 0.1 g of spearmint sample was resuspended in 1 mL of extract solution, shortly vortexed and centrifuged at 8000 *g* for 10 min at 4°C. After that, the supernatant was collected, and OD was measured at 290 nm using a TECAN Spectrometer (Infinite 200 PRO plate reader). Results were expressed as unit of enzyme activity per gram of fresh plant tissue

(U/g FW). Cinnamyl alcohol dehydrogenase (CAD) activity was determined using a specific kit (BC0205, Solarbio Science and Technology Co. Ltd., Beijing, China). Briefly, 1 mL of extract solution was used to resuspend 0.1 g of spearmint powder. The sample was vortexed and centrifuged at 10 000 *g* for 10 min at 4°C; then, the supernatant was collected in a new tube and diluted with all the reagents, as reported in the manufacturer's guidelines. At the end, OD was spectrophotometrically determined at 340 nm (Infinite 200 PRO plate reader, TECAN) and CAD activity was expressed as unit of enzyme per gram of fresh plant weight (U/g FW). POD activity was estimated using another kit (BC0095, Solarbio Science and Technology Co. Ltd., Beijing, China). One hundred mg of plant material was mixed with 1 mL of the extract solution. The sample was centrifuged at 8 000 *g* for 10 min at 4°C, and the supernatant was collected and maintained on ice until testing. Reagents were added as per protocol. The OD value was determined at 470 nm using a spectrophotometer (microplate reader Sunrise, Tecan) and POD activity was reported as unit of enzyme per gram of fresh plant weight (U/g FW).

4.9 | Lignin Content

Total lignin content was evaluated by a specific kit (BC4205, Solarbio Science & Technology Co. Ltd., Beijing, China), following the protocol guidelines. Briefly, plant powdered material was totally dried at 80°C to reach a constant weight. Then, 3 mg were weighed into a 1.5 mL Eppendorf tube and subjected to the several steps of the spectrophotometric assay. Lignin content was expressed as milligrams per gram of fresh plant weight (mg/g FW), then expressed as percentage content of lignin (%).

4.10 | Chromatographic Analysis

Following the protocol of Kao et al. (2024) with some modifications, 100 mg of plant material was dissolved in 0.5 mL of extraction buffer (ACN:acetone:MeOH:H_2O = 1:1:1:1, v/v/v/v) for 12 h, under agitation, in the dark at 4°C. After centrifugation at 13 000 *g* for 10 min at 4°C, the supernatant was collected and dried at 40°C with an Eppendorf Concentrator Plus. The pellet was then resuspended in 100 μL of MeOH:H_2O (50:50; v/v) and then subjected to liquid chromatography for targeted compound analysis. An HPLC system was employed to measure the content of specific phenolic compounds, monolignols, in each extract. The instrument was provided with a CBM-20A controller, an LC-20 AD pump, a SIL-20a HT autosampler, and an SPDM20A diode array detector (DAD) (Shimadzu, Kyoto, Japan). A Luna 3u C18 (Alonso-Peral et al. 2010) column (150 × 4.60 mm × 3 μm) (Phenomenex, Torrance, CA, USA) and two mobile phases, consisting of 1% formic acid (v/v) (phase A) and methanol (phase B) at a flow rate of 0.95 mL per minute, were used for the chromatographic separation. Column temperature was set at 40°C, while the elution gradient was set as follows: it began at 15% solvent B and remained constant for 20 min; then, solvent B was linearly increased up to 35% in 20 min and up to 90% in 55 min. At 70 min, the solvent B was reported at the initial condition. LABSOLUTION software (Shimadzu) was used for data acquisition. Monolignols (i.e., *p*-coumaryl alcohol, coniferyl alcohol and sinapyl alcohol) were detected in the extracts at 260 nm. Each metabolite was analysed in quantitative terms, comparing their retention times (minutes), absorption spectra, and peak areas with those of pure standard molecules (Sigma-Aldrich, Milan, Italy). Results were indicated as percentage variation with respect to the CNT sample, set at 100%.

4.11 | In Vitro Antioxidant Tests

FRAP (2,4,6-tris 2-pyridyl-s-triazine; Sigma Aldrich) and ABTS (2,20-azino-bis-3- ethylbenzothiazoline-6-sulfonic acid; Sigma-Aldrich) assays were carried out to determine the total antiradical status of spearmint tissues, according to Gismondi et al. (2018). In both these spectrophotometric tests, ascorbic acid (AA) was used as reference to obtain a calibration curve (0–30 mg/L). The absorbance of the solutions was measured at 593 nm for FRAP and 734 nm for ABTS experiments. Results (i.e., free radical scavenging activity) were expressed as micromoles of AAE per mg of fresh plant weight (μmol AAE/mg FW).

4.12 | Statistics

Each experimental point consisted of 6 different plants, as already reported above, and all experiments were carried out in triplicate (technical replicates) on the plant material obtained from each of them (independent biological replicates, $n = 6$). Results were reported as means ± standard deviation (SD) or percentage. Two-way ANOVA test was used for statistical analysis, and the differences were evaluated by the post hoc lowest standard deviations (LSD) test, through Microsoft Excel software. In the graphs, different letters on the columns indicate significant differences with a $p < 0.05$.

Author Contributions

Conceptualization: A.G.; investigation: A.D., A.T., C.P., G.P. and G.D.M.; validation: A.G., G.P., M.H.-C., and A.D.; data curation: A.D., and A.G.; writing – original draft preparation: A.D., and A.G.; writing – review and editing: all authors; supervision: A.G., M.H.-C. and A.C.; resources: A.G. and A.C.

Acknowledgements

The authors want to thank Lorenzo Olmi for his assistance during plant treatments.

Funding

This work was carried out as part of the activities of the National Center for Gene Therapy and Drugs based on RNA Technology, funded in the framework of the National Recovery and Resilience Plan (PNRR), Mission 4 "Education and Research", Component 2 "From Research to Business", Investment 1.4 "Strengthening research structures for supporting the creation of National Centres, national R&D leaders on some Key Enabling Technologies", funded by the European Union—Next Generation EU, Project CN00000041, CUP B93D21010860004, Spoke 7 "National Center for Gene Therapy and Drugs based on RNA Technology."

Conflicts of Interest

The authors declare no conflicts of interest.

Data Availability Statement

All data reported in this article are present in the manuscript or in the relative supplemental materials. Raw data of small-RNA sequencing are available in the repository ZENODO (https://doi.org/10.5281/zenodo.18863040).

References

Abdel-Ghany, S. E., and M. Pilon. 2008. "MicroRNA-Mediated Systemic Down-Regulation of Copper Protein Expression in Response to Low Copper Availability in *Arabidopsis*." *Journal of Biological Chemistry* 283: 15932–15945.

Alonso-Peral, M. M., J. Li, Y. Li, et al. 2010. "The microRNA159-Regulated GAMYB-Like Genes Inhibit Growth and Promote Programmed Cell Death in *Arabidopsis*." *Plant Physiology* 154: 757–771.

Andrews, S. 2010. *FastQC: A Quality Control Tool for High Throughput Sequence Data*. Babraham Institute. http://www.bioinformatics.babraham.ac.uk/projects/fastqc/.

Arcuri, M. L. C., L. C. Fialho, A. V. Nunes-Laitz, et al. 2020. "Genome-Wide Identification of Multifunctional Laccase Gene Family in *Eucalyptus grandis*: Potential Targets for Lignin Engineering and Stress Tolerance." *Trees* 34: 745–758.

Arif, A., C. Chahel, S. Zeng, et al. 2018. "Plant-Specific Transcription Factor LrTCP4 Enhances Secondary Metabolite Biosynthesis in *Lycium ruthenicum* Hairy Roots." *Plant Cell, Tissue and Organ Culture* 136: 2. https://doi.org/10.1007/s11240-018-1518-2.

Arslan, E., G. Agar, and M. Aydin. 2021. "Humic Acid as a Biostimulant in Improving Drought Tolerance in Wheat: The Expression Patterns of Drought-Related Genes." *Plant Molecular Biology Reporter* 39: 508–519.

Barros, J., H. Serk, I. Granlund, and E. Pesquet. 2015. "The Cell Biology of Lignification in Higher Plants." *Annals of Botany* 115: 1053–1074.

Basso, M. F., P. C. G. Ferreira, A. K. Kobayashi, et al. 2019. "MicroRNAs and New Biotechnological Tools for Their Modulation and Improving Stress Tolerance in Plants." *Plant Biotechnology Journal* 17: 1482–1500.

Begum, Y. 2022. "Regulatory Role of microRNAs (miRNAs) in the Recent Development of Abiotic Stress Tolerance of Plants." *Gene* 821: 146283.

Boerjan, W., J. Ralph, and M. Baucher. 2003. "Lignin Biosynthesis." *Annual Review of Plant Biology* 54: 519–546.

Bonawitz, N. D., and C. Chapple. 2010. "The Genetics of Lignin Biosynthesis: Connecting Genotype to Phenotype." *Annual Review of Genetics* 44: 337–363.

Bulgari, R., G. Franzoni, and A. Ferrante. 2019. "Biostimulants Application in Horticultural Crops Under Abiotic Stress Conditions." *Agronomy* 9: 306.

Bushnell, B. 2014. "BBMap: A Fast, Accurate, Splice-Aware Aligner."

Cao, Y., Y. Mei, R. Zhang, et al. 2024. "Transcriptional Regulation of Flavonol Biosynthesis in Plants." *Horticultural Research* 11: uhae043.

Challa, K. R., P. Aggarwal, and U. Nath. 2016. "Activation of YUCCA5 by the Transcription Factor TCP4 Integrates Developmental and Environmental Signals to Promote Hypocotyl Elongation in *Arabidopsis*." *Plant Cell* 28: 2117–2130.

Chen, H., Z. Li, and L. Xiong. 2012. "A Plant microRNA Regulates the Adaptation of Roots to Drought Stress." *FEBS Letters* 586: 1742–1747.

Chinnusamy, V., J. Zhu, T. Zhou, and J. K. Zhu. 2007. "Small RNAs: Big Role in Abiotic Stress Tolerance of Plants." In: *Advances in Molecular Breeding* (Jenks MA, Hasegawa PM, Jain SM, eds), 223–260. Springer.

Choi, S. J., Z. Lee, S. Kim, and J. S. Shim. 2023. "Modulation of Lignin Biosynthesis for Drought Tolerance in Plants." *Frontiers in Plant Science* 14: 1116426.

Covarrubias, A. A., and J. L. Reyes. 2010. "Post-Transcriptional Gene Regulation of Salinity and Drought Responses by Plant microRNAs." *Plant, Cell & Environment* 33: 481–489.

Cui, M. H., K. S. Yoo, S. Hyoung, et al. 2013. "An *Arabidopsis* R2R3-MYB Transcription Factor, AtMYB20, Negatively Regulates Type 2C Serine/Threonine Protein Phosphatases to Enhance Salt Tolerance." *FEBS Letters* 587: 1773–1778.

D'Agostino, A., G. Di Marco, A. Canini, and A. Gismondi. 2024. "Gallic Acid as a Phytostimulant Enhancing Yield and Quality of *Mentha spicata* L. Under Well- and Deficit-Watered Conditions." *Environmental and Experimental Botany* 219: 105–106.

D'Agostino, A., G. Di Marco, A. Canini, and A. Gismondi. 2025. "Exogenous Gallic Acid Induces Changes in the Metabolome of *Mentha arvensis* L. Regulating the Expression of Key Genes Involved in Menthol Biosynthesis." *Scientia Horticulturae* 350: 114282.

Dai, X., and P. X. Zhao. 2011. "psRNATarget: A Plant Small RNA Target Analysis Server." *Nucleic Acids Research* 39: W155–W159.

Dai, X., Z. Zhuang, and P. X. Zhao. 2018. "psRNATarget: A Plant Small RNA Target Analysis Server." *Nucleic Acids Research* 46, no. W1: W49–W54.

Daszkowska-Golec, A., and I. Szarejko. 2013. "The Molecular Basis of ABA-Mediated Plant Response to Drought." In *Abiotic Stress–Plant Responses and Applications in Agriculture*, 103–134. IntechOpen.

Delfine, S., F. Loreto, P. Pinelli, R. Tognetti, and A. Alvino. 2005. "Isoprenoids Content and Photosynthetic Limitations in Rosemary and Spearmint Plants Under Water Stress." *Agriculture, Ecosystems & Environment* 106: 243–252.

Di Marco, G., A. Gismondi, L. Panzanella, et al. 2018. "Botanical Influence on Phenolic Profile and Antioxidant Level of Italian Honeys." *Journal of Food Science and Technology* 55: 4042–4050.

Ding, Y., Y. Tao, and C. Zhu. 2013. "Emerging Roles of microRNAs in the Mediation of Drought Stress Response in Plants." *Journal of Experimental Botany* 64: 3077–3086.

Dong, C.-H., and H. Pei. 2014. "Over-Expression of miR397 Improves Plant Tolerance to Cold Stress in *Arabidopsis thaliana*." *Journal of Plant Biology* 57: 209–217.

Drobek, M., M. Frac, and J. Cybulska. 2019. "Plant Biostimulants: Importance of the Quality and Yield of Horticultural Crops and Improvement of Plant Tolerance to Abiotic Stress—A Review." *Agronomy* 9: 335.

Eldem, V., U. C. Akcay, E. Ozhuner, Y. Bakir, S. Uranbey, and T. Unver. 2012. "Genome-Wide Identification of miRNAs Responsive to Drought in Peach (*Prunus persica*) by High-Throughput Deep Sequencing." *PLoS One* 7: e50298.

Ferdous, J., S. S. Hussain, and B. J. Shi. 2015. "Role of microRNAs in Plant Drought Tolerance." *Plant Biotechnology Journal* 13: 293–305.

Gaddam, S. R., C. Bhatia, H. Gautam, et al. 2022. "Ethylene Regulates miRNA-Mediated Lignin Biosynthesis and Leaf Serration in *Arabidopsis thaliana*." *Biochemical and Biophysical Research Communications* 605: 51–55.

Gao, Y., B. Feng, C. Gao, et al. 2022. "The Evolution and Functional Roles of miR408 and Its Targets in Plants." *International Journal of Molecular Sciences* 23: 530.

Gayoso, C., F. Pomar, E. Novo-Uzal, F. Merino, and Ó. de Martínez Ilárduya. 2010. "The Ve-Mediated Resistance Response of the Tomato to *Verticillium dahliae* Involves H_2O_2, Peroxidase and Lignins and Drives PAL Gene Expression." *BMC Plant Biology* 10: 232.

Geng, P., S. Zhang, J. Liu, et al. 2020. "MYB20, MYB42, MYB43, and MYB85 Regulate Phenylalanine and Lignin Biosynthesis During Secondary Cell Wall Formation." *Plant Physiology* 182: 1272–1283.

Gismondi, A., L. Canuti, S. Impei, et al. 2013. "Antioxidant Extracts of African Medicinal Plants Induce Cell Cycle Arrest and Differentiation in B16F10 Melanoma Cells." *International Journal of Oncology* 43: 956–964.

Gismondi, A., S. De Rossi, L. Canuti, et al. 2018. "From *Robinia pseudoacacia* L. Nectar to Acacia Monofloral Honey: Biochemical Changes and Variation of Biological Properties." *Journal of the Science of Food and Agriculture* 98: 4312–4322.

Gismondi, A., G. Di Marco, and A. Canini. 2017. "Detection of Plant microRNAs in Honey." *PLoS One* 12: e0172981.

Guleria, P., M. Mahajan, J. Bhardwaj, and S. K. Yadav. 2011. "Plant Small RNAs: Biogenesis, Mode of Action and Their Roles in Abiotic Stresses." *Genomics, Proteomics & Bioinformatics* 9: 183–199.

Guo, X., A. Ullah, D. Siuta, B. Kukfisz, and S. Iqbal. 2022. "Role of WRKY Transcription Factors in Regulation of Abiotic Stress Responses in Cotton." *Life* 12: 1410.

Hanks, S. K., and T. Hunter. 1995. "The Eukaryotic Protein Kinase Superfamily: Kinase (Catalytic) Domain and Classification." *FASEB Journal* 9: 576–596.

Hao, K., Y. Wang, Z. Zhu, Y. Wu, R. Chen, and L. Zhang. 2022. "miR160: An Indispensable Regulator in Plant." *Frontiers in Plant Science* 13: 833322.

Huang, S., J. Zhou, L. Gao, and Y. Tang. 2020. "Plant miR397 and Its Functions." *Functional Plant Biology* 48: 361–370.

Hussain, Q., M. Asim, R. Zhang, R. Khan, S. Farooq, and J. Wu. 2021. "Transcription Factors Interact With ABA Through Gene Expression and Signaling Pathways Tomitigate Drought and Salinity Stress." *Biomolecules* 11: 1159.

Islam, W., A. Idrees, A. Waheed, and F. Zeng. 2022. "Plant Responses to Drought Stress: microRNAs in Action." *Environmental Research* 215: 114282.

Jones-Rhoades, M. W., and D. P. Bartel. 2004. "Computational Identification of Plant microRNAs and Their Targets, Including a Stress-Induced miRNA." *Molecular Cell* 14: 787–799.

Kao, C. T., F. W. Yang, M. C. Wu, et al. 2024. "Systematic Synthesis and Identification of Monolignol Pathway Metabolites." *New Phytologist* 244: 1143–1167.

Khan, S. A., M. Z. Li, S. M. Wang, and H. J. Yin. 2018. "Revisiting the Role of Plant Transcription Factors in the Battle Against Abiotic Stress." *International Journal of Molecular Sciences* 19: 1634.

Khandal, H., A. P. Singh, and D. Chattopadhyay. 2020. "The MicroRNA397b-LACCASE2 Module Regulates Root Lignification Under Water and Phosphate Deficiency." *Plant Physiology* 182: 1387–1403.

Kim, J. S., K. Mochida, and K. Shinozaki. 2022. "ER Stress and the Unfolded Protein Response: Homeostatic Regulation Coordinate Plant Survival and Growth." *Plants* 11: 3197.

Kitin, P., S. L. Voelker, F. C. Meinzer, H. Beeckman, S. H. Strauss, and B. Lachenbruch. 2010. "Tyloses and Phenolic Deposits in Xylem Vessels Impede Water Transport in Low-Lignin Transgenic Poplars: A Study by Cryo-Fluorescence Microscopy." *Plant Physiology* 154: 887–898.

Kodama, Y., N. Suetsugu, S. G. Kong, and M. Wada. 2010. "Two Interacting Coiled-Coil Proteins, WEB1 and PMI2, Maintain the Chloroplast Photorelocation Movement Velocity in Arabidopsis." *Proceedings of the National Academy of Sciences of the United States of America* 107: 19591–19596.

Kozomara, A., M. Birgaoanu, and S. Griffiths-Jones. 2019. "miRBase: From microRNA Sequences to Function." *Nucleic Acids Research* 47: D155–D162.

Legay, S., G. Guerriero, C. André, et al. 2016. "MdMyb93 Is a Regulator of Suberin Deposition in Russeted Apple Fruit Skins." *New Phytologist* 212: 977–991.

Lewis, D. R., M. V. Ramirez, N. D. Miller, et al. 2011. "Auxin and Ethylene Induce Flavonol Accumulation Through Distinct Transcriptional Networks." *Plant Physiology* 156: 144–164.

Li, W., and A. Godzik. 2006. "Cd-Hit: A Fast Program for Clustering and Comparing Large Sets of Protein or Nucleotide Sequences." *Bioinformatics* 22: 1658–1659.

Li, W., S. Pang, Z. Lu, and B. Jin. 2020. "Function and Mechanism of WRKY Transcription Factors in Abiotic Stress Responses of Plants." *Plants* 9: 1515.

Li, Y., M. Alonso-Peral, G. Wong, M.-B. Wang, and A. A. Millar. 2016. "Ubiquitous miR159 Repression of MYB33/65 in *Arabidopsis* Rosettes Is Robust and Is Not Perturbed by a Wide Range of Stresses." *BMC Plant Biology* 16: 179.

Liang, K., Y. Chen, J. Hou, F. Yan, and F. Liu. 2024. "ABA-Mediated Stomatal Response Modulates the Effects of Drought, Salinity and Combined Stress on Tomato Plants Grown Under Elevated CO_2." *Environmental and Experimental Botany* 223: 105797.

Liang, R., L. You, F. Dong, X. Zhao, and J. Zhao. 2020. "Identification of Hydroxyproline-Containing Proteins and Hydroxylation of Proline Residues in Rice." *Frontiers in Plant Science* 11: 1207.

Liang, Y., X. Yang, C. Wang, and Y. Wang. 2024. "miRNAs: Primary Modulators of Plant Drought Tolerance." *Journal of Plant Physiology* 301: 154313.

Liu, F., Y. Tang, Q. Guo, and J. Chen. 2020. "Identification and Characterization of microRNAs in Phloem and Xylem From Ramie (*Boehmeria nivea*)." *Molecular Biology Reports* 47: 1013–1020.

Liu, P. P., T. A. Montgomery, N. Fahlgren, K. D. Kasschau, H. Nonogaki, and J. C. Carrington. 2007. "Repression of AUXIN RESPONSE FACTOR10 by microRNA160 Is Critical for Seed Germination and Post-Germination Stages." *Plant Cell* 19: 1897–1910.

Liu, Q., L. Luo, and L. Zheng. 2018. "Lignins: Biosynthesis and Biological Functions in Plants." *International Journal of Molecular Sciences* 19: 1–16.

Liu, X., X. Dong, Z. Liu, et al. 2016. "Repression of ARF10 by microRNA160 Plays an Important Role in the Mediation of Leaf Water Loss." *Plant Molecular Biology* 92: 313–336.

Liu, Y., Y. Qiao, and W. Liao. 2025. "Calmodulin-Binding Transcription Factors: Roles in Plant Response to Abiotic Stresses." *Plants* 14: 532.

Love, M. I., W. Huber, and S. Anders. 2014. "Moderated Estimation of Fold Change and Dispersion for RNA-Seq Data With DESeq2." *Genome Biology* 15: 550.

Lu, S., Q. Li, H. Wei, et al. 2013. "Ptr-miR397a Is a Negative Regulator of Laccase Genes Affecting Lignin Content in *Populus trichocarpa*." *Proceedings of the National Academy of Sciences of the United States of America* 110: 10848–10853.

Lu, Y., Z. Feng, X. Liu, et al. 2018. "miR393 and miR390 Synergistically Regulate Lateral Root Growth in Rice Under Different Conditions." *BMC Plant Biology* 18: 1–12.

Mallory, A. C., D. P. Bartel, and B. Bartel. 2005. "MicroRNA-Directed Regulation of Arabidopsis AUXIN RESPONSE FACTOR17 Is Essential for Proper Development and Modulates Expression of Early Auxin Response Genes." *Plant Cell* 17: 1360–1375.

Marino, S., U. Ahmad, M. I. Ferreira, and A. Alvino. 2019. "Evaluation of the Effect of Irrigation on Biometric Growth, Physiological Response, and Essential Oil of *Mentha spicata* L." *Water* 11: 2264.

Martin, M. 2011. "Cutadapt Removes Adapter Sequences From High-Throughput Sequencing Reads." *EMBnet.Journal* 17: 10–12.

McCarthy, R. L., R. Zhong, and Z. H. Ye. 2009. "MYB83 Is a Direct Target of SND1 and Acts Redundantly With MYB46 in the Regulation of Secondary Cell Wall Biosynthesis in *Arabidopsis*." *Plant and Cell Physiology* 50: 1950–1964.

Millar, A. A., A. Lohe, and G. Wong. 2019. "Biology and Function of miR159 in Plants." *Plants* 8: 255.

Mittler, R., S. I. Zandalinas, Y. Fichman, and F. Van Breusegem. 2022. "Reactive Oxygen Species Signalling in Plant Stress Responses." *Nature Reviews. Molecular Cell Biology* 23: 663–679.

Morad-Talab, N., and R. Hajiboland. 2016. "MicroRNAs and Their Role in Drought Stress Response in Plants." In *Water Stress and Crop Plants: A Sustainable Approach*, 261–286. John Wiley & Sons, Ltd.

Moura-Sobczak, J. C. M. S., U. Souza, and P. Mazzafera. 2011. "Drought Stress and Changes in the Lignin Content and Composition in Eucalyptus." *BMC Proceedings* 5, no. S7: P103.

Nakabayashi, R., K. Yonekura-Sakakibara, K. Urano, et al. 2014. "Enhancement of Oxidative and Drought Tolerance in *Arabidopsis* by Overaccumulation of Antioxidant Flavonoids." *Plant Journal* 77: 367–379.

Navarro, L., P. Dunoyer, F. Jay, et al. 2006. "A Plant miRNA Contributes to Antibacterial Resistance by Repressing Auxin Signaling." *Science* 312: 436–439.

Niu, Z., G. Li, H. Hu, et al. 2021. "A Gene That Underwent Adaptive Evolution, LAC2 (LACCASE), in Populus Euphratica Improves Drought Tolerance by Improving Water Transport Capacity." *Horticultural Research* 8: 1–12.

Parry, G., and M. Estelle. 2006. "Auxin Receptors: A New Role for F-Box Proteins." *Current Opinion in Cell Biology* 18: 152–156.

Peng, X., C. Feng, Y. T. Wang, et al. 2022. "miR164g-MsNAC022 Acts as a Novel Module Mediating Drought Response by Transcriptional Regulation of Reactive Oxygen Species Scavenging Systems in Apple." *Horticulture Research* 9: uhac192.

Pesquet, E., A. Wagner, and J. H. Grabber. 2019. "Cell Culture Systems: Invaluable Tools to Investigate Lignin Formation and Cell Wall Properties." *Current Opinion in Biotechnology* 56: 215–222.

Ralph, J., K. Lundquist, G. Brunow, et al. 2004. "Lignins: Natural Polymers From Oxidative Coupling of 4-Hydroxyphenyl-Propanoids." *Phytochemistry Reviews* 3: 29–60.

Reyes, J. L., and N. H. Chua. 2007. "ABA Induction of miR159 Controls Transcript Levels of Two MYB Factors During *Arabidopsis* Seed Germination." *Plant Journal* 49: 592–606.

Samad, N. A. F., M. Sajad, N. Nazaruddin, et al. 2017. "MicroRNA and Transcription Factor: Key Players in Plant Regulatory Network." *Frontiers in Plant Science* 8: 565.

Şanlı, B. A., and Z. N. Öztürk Gökçe. 2021. "Investigating Effect of miR160 Through Overexpression in Potato Cultivars Under Single or Combination of Heat and Drought Stresses." *Plant Biotechnology Reports* 15: 335–348.

Sarkanen, S., R. A. Razal, T. Piccariello, E. Yamamoto, and N. G. Lewis. 1991. "Lignin Peroxidase: Toward a Clarification of Its Role In Vivo." *Journal of Biological Chemistry* 266: 3636–3643.

Sharma, N. K., S. K. Gupta, V. Dwivedi, and D. Chattopadhyay. 2020. "Lignin Deposition in Chickpea Root Xylem Under Drought." *Plant Signaling & Behavior* 15: 1754621.

Sharma, P., A. B. Jha, R. S. Dubey, and M. Pessarakli. 2012. "Reactive Oxygen Species, Oxidative Damage, and Antioxidative Defense Mechanism in Plants Under Stressful Conditions." *Journal of Botany* 2012: 217037.

Shi, H., L. Chen, T. Ye, X. Liu, K. Ding, and Z. Chan. 2014. "Modulation of Auxin Content in *Arabidopsis* Confers Improved Drought Stress Resistance." *Plant Physiology and Biochemistry* 82: 209–217.

Shkryl, Y., Z. Tsydeneshieva, A. Degtyarenko, et al. 2022. "Plant Exosomal Vesicles: Perspective Information Nanocarriers in Biomedicine." *Applied Sciences* 12: 8262.

Showalter, A. M., B. D. Keppler, X. Liu, J. Lichtenberg, and L. R. Welch. 2016. "Bioinformatic Identification and Analysis of Hydroxyproline-Rich Glycoproteins in *Populus trichocarpa*." *BMC Plant Biology* 16: 229.

Subha, D., R. AnuKiruthika, H. Sreeraj, and K. S. Tamilselvi. 2023. "Plant Exosomes: Nano Conveyors of Pathogen Resistance." *Discover Nano* 18: 146.

Sunkar, R., Y. F. Li, and G. Jagadeeswaran. 2012. "Functions of microRNAs in Plant Stress Responses." *Trends in Plant Science* 17: 196–203.

Sunkar, R., and J. K. Zhu. 2004. "Novel and Stress-Regulated microRNAs and Other Small RNAs From *Arabidopsis*." *Plant Cell* 16: 2001–2019.

Swetha, C., D. Basu, K. Pachamuthu, et al. 2018. "Major Domestication-Related Phenotypes in *Indica* Rice Are due to Loss of miRNA-Mediated Laccase Silencing." *Plant Cell* 30: 2649–2662.

Tang, D., M. Chen, X. Huang, et al. 2023. "SRplot: A Free Online Platform for Data Visualization and Graphing." *PLoS One* 18: e0294236.

Tiwari, R., and M. V. Rajam. 2022. "RNA- and miRNA-Interference to Enhance Abiotic Stress Tolerance in Plants." *Journal of Plant Biochemistry and Biotechnology* 31: 689–704.

Turlapati, P. V., K. W. Kim, L. B. Davin, and N. G. Lewis. 2011. "The Laccase Multigene Family in *Arabidopsis thaliana*: Towards Addressing the Mystery of Their Gene Functions." *Planta* 233: 439–470.

Ulmasov, T., G. Hagen, and T. J. Guilfoyle. 1999. "Activation and Repression of Transcription by Auxin-Response Factors." *Proceedings. National Academy of Sciences. United States of America* 96: 5844–5849.

Vanholme, R., B. Demedts, K. Morreel, J. Ralph, and W. Boerjan. 2010. "Lignin Biosynthesis and Structure." *Plant Physiology* 153: 895–905.

Wang, B., M. Du, N. Liu, N. Sun, and X. Qi. 2013. "*Arabidopsis* Transcription Factor WRKY33 Is Involved in Drought by Directly Regulating the Expression of CesA8." *American Journal of Plant Sciences* 4: 21–27.

Wang, B., N. Song, Q. Zhang, N. Wang, and Z. Kang. 2018. "TaMAPK4 Acts as a Positive Regulator in Defense of Wheat Stripe-Rust Infection." *Frontiers in Plant Science* 9: 152.

Wang, C.-Y., S. Zhang, Y. Yu, et al. 2014. "miR397b Regulates Both Lignin Content and Seed Number in *Arabidopsis* via Modulating a Laccase Involved in Lignin Biosynthesis." *Plant Biotechnology Journal* 12: 1132–1142.

Wang, F., W. Kong, G. Wong, et al. 2016. "AtMYB12 Regulates Flavonoid Accumulation and Abiotic Stress Tolerance in Transgenic *Arabidopsis thaliana*." *Molecular Genetics and Genomics* 291: 1545–1559.

Wang, N. N., S. W. Xu, Y. L. Sun, et al. 2019. "The Cotton WRKY Transcription Factor (GhWRKY33) Reduces Transgenic *Arabidopsis* Resistance to Drought Stress." *Scientific Reports* 9: 724.

Wang, X., Y. Niu, and Y. Zheng. 2021. "Multiple Functions of MYB Transcription Factors in Abiotic Stress Responses." *International Journal of Molecular Sciences* 22: 6125.

Weng, J. K., and C. Chapple. 2010. "The Origin and Evolution of Lignin Biosynthesis." *New Phytologist* 187: 273–285.

Windels, D., D. Bielewicz, M. Ebneter, A. Jarmolowski, Z. Szweykowska-Kulinska, and F. Vazquez. 2014. "miR393 Is Required for Production of Proper Auxin Signalling Outputs." *PLoS One* 9: e95972.

Wu, G., M. Y. Park, S. R. Conway, J. W. Wang, D. Weigel, and R. S. Poethig. 2009. "The Sequential Action of miR156 and miR172 Regulates Developmental Timing in *Arabidopsis*." *Cell* 138: 750–759.

Wyrzykowska, A., D. Bielewicz, P. Plewka, et al. 2022. "The MYB33, MYB65, and MYB101 Transcription Factors Affect *Arabidopsis* and Potato Responses to Drought by Regulating the ABA Signaling Pathway." *Physiologia Plantarum* 174: e13775.

Yadav, S., and D. Chattopadhyay. 2023. "Lignin: The Building Block of Defense Responses to Stress in Plants." *Journal of Plant Growth Regulation* 42: 6652–6666.

Yan, C., Z. Hu, Z. Nie, J. Li, X. Yao, and H. Yin. 2021. "CcBLH6, a Bell-Like Homeodomain-Containing Transcription Factor, Regulates the Fruit Lignification Pattern." *Planta* 253: 90.

Yang, T., Y. Wang, S. Teotia, et al. 2019. "The Interaction Between miR160 and miR165/166 in the Control of Leaf Development and Drought Tolerance in *Arabidopsis*." *Scientific Reports* 9: 2832.

Yu, Y. 2020. "LACCASE2 Negatively Regulates Lignin Deposition of *Arabidopsis* Roots." *Plant Physiology* 182: 1190–1191.

Zhang, B. 2015. "MicroRNA: A New Target for Improving Plant Tolerance to Abiotic Stress." *Journal of Experimental Botany* 66: 1749–1761.

Zhang, J., and M. B. Kirkham. 1994. "Drought-Stress-Induced Changes in Activities of Superoxide Dismutase, Catalase, and Peroxidase in Wheat Species." *Plant and Cell Physiology* 35: 785–791.

Zhang, L. L., Y. Chen, Z. J. Li, X. Li, and G. Fan. 2022. "Bioactive Properties of the Aromatic Molecules of Spearmint (*Mentha spicata* L.) Essential Oil: A Review." *Food & Function* 13: 3110–3132.

Zhang, Y., X. Shan, Q. Zhao, and F. Shi. 2022. "The microRNA397a-LACCASE17 Module Regulates Lignin Biosynthesis in *Medicago ruthenica* (L.)." *Frontiers in Plant Science* 13: 978515.

Zhang, Y.-C., Y. Yu, C.-Y. Wang, et al. 2013. "Overexpression of microRNA OsmiR397 Improves Rice Yield by Increasing Grain Size and Promoting Panicle Branching." *Nature Biotechnology* 31: 848.

Zhao, Q., and R. A. Dixon. 2011. "Transcriptional Networks for Lignin Biosynthesis: More Complex Than We Thought?" *Trends in Plant Science* 16: 227–233.

Zhen Li, Z., F. Liang, T. Zhang, N. Fu, X. Pei, and Y. Long. 2021. "Enhanced Tolerance to Drought Stress Resulting From *Caragana korshinskii* CkWRKY33 in Transgenic *Arabidopsis thaliana*." *BMC Genomic Data* 22: 11.

Zhong, R., C. Lee, R. L. McCarthy, C. K. Reeves, E. G. Jones, and Z. H. Ye. 2011. "Transcriptional Activation of Secondary Wall Biosynthesis by Rice and Maize NAC and MYB Transcription Factors." *Plant and Cell Physiology* 52: 1856–1871.

Zhou, J., C. Lee, R. Zhong, and Z. H. Ye. 2009. "MYB58 and MYB63 Are Transcriptional Activators of the Lignin Biosynthetic Pathway During Secondary Cell Wall Formation in *Arabidopsis*." *Plant Cell* 21: 248–266.

Zhou, L., Y. Liu, Z. Liu, D. Kong, M. Duan, and L. Luo. 2010. "Genome-Wide Identification and Analysis of Drought-Responsive microRNAs in *Oryza sativa*." *Journal of Experimental Botany* 61: 4157–4168.

Zhou, M., D. Li, Z. Li, et al. 2013. "Constitutive Expression of a miR319 Gene Alters Plant Development and Enhances Salt and Drought Tolerance in Transgenic Creeping Bentgrass." *Plant Physiology* 161: 1375–1391.

Zhou, Y., B. Zhou, L. Pache, et al. 2019. "Metascape Provides a Biologist-Oriented Resource for the Analysis of Systems-Level Datasets." *Nature Communications* 10: 1523.

Supporting Information

Additional supporting information can be found online in the Supporting Information section. **Data S1:** Primers used for qRT-PCR experiments. **Data S2:** Raw data of the bioinformatics prediction by psRNATarget relative to DEMs' targets. For each DEM, the list of predicted targets was reported. For each one of these targets, accession ID, expectation value, UPE, miRNA start nucleotide, miRNA end nucleotide, target start nucleotide, target end nucleotide, miRNA aligned fragment, alignment representation, target aligned fragment, type of inhibition activity, target description, and multiplicity were listed.